



# A regularization method to improve adversarial robustness of neural networks for ECG signal classification

Linhai Ma, Liang Liang\*

*Department of Computer Science, University of Miami, Coral Gables, FL, USA*



## ARTICLE INFO

**Keywords:**  
ECG signal classification  
Deep neural network  
Adversarial robustness  
Adversarial noise

## ABSTRACT

With the advancement of machine learning technologies, Deep Neural Networks (DNNs) have been utilized for automated interpretation of Electrocardiogram (ECG) signals to identify potential abnormalities in a patient's heart within a second. Studies have shown that the accuracy of DNNs for ECG signal classification could reach human-expert cardiologist level if a sufficiently large training dataset is available. However, it is known that, in the field of computer vision, DNNs are not robust to adversarial noises that may cause DNNs to make wrong class-label predictions. In this work, we confirm that DNNs are not robust to adversarial noises in ECG signal classification applications, and we propose a novel regularization method to improve DNN robustness by minimizing the noise-to-signal ratio. Our method is evaluated on two public datasets: the MIT-BIH dataset and the CPSC2018 dataset, and the evaluation results show that our method can significantly enhance DNN robustness against adversarial noises generated by Projected Gradient Descent (PGD) and Smooth Adversarial Perturbation (SAP) adversarial attacks, with a minimal reduction of accuracy on clean data. Our method may serve as the baseline for designing new methods to defend against adversarial attacks for life-critical applications depending on ECG interpretation. The code of this work is publicly available at [github.com/SarielMa/Robust\\_DNN\\_for\\_ECG](https://github.com/SarielMa/Robust_DNN_for_ECG).

## 1. Introduction

Electrocardiogram (ECG) is often the first step for the diagnosis of heart conditions before using expensive cardiac medical imaging. With the rapid development of embedded systems and sensor technologies, portable and wearable ECG devices are increasingly used to monitor patient conditions on a daily basis. The amount of ECG data collected by these devices may have exceeded the capacity of human cardiologists. For patients in the developing countries where human cardiologists are lacking, computational methods, such as machine learning, may provide an accessible and affordable solution for automated ECG signal analysis, e.g., classifying ECG signals into different disease categories.

Researchers have been developing machine learning-based ECG signal analysis methods for decades. Among the machine learning techniques, Deep Neural Networks (DNNs), including Convolutional Neural Networks (CNNs), have demonstrated superior performance in a wide range of applications [1] and were successfully applied for ECG signal classification [2–4]. The first work of using CNN for ECG signal classification was reported by S. Kiranyaz et al., in 2015 [5], in which an adaptive one-dimensional (1D) CNN was designed for ECG classification

on the MIT-BIH dataset. Notably, Awni Y. Hannun et al., in 2017 [6] developed a CNN to classify 12 rhythm classes using a dataset of 91,232 single-lead ECGs from 53,877 patients, which is the largest (yet private) dataset compared to other public datasets, and the classification accuracy was similar to that of human-expert cardiologists. Thus, with a sufficiently large amount of data and a carefully designed structure, the trained DNN model could reach the human-expert level for ECG signal classification. For a complete list of DNNs for ECG signal analysis, we refer the reader to the review [4] that summarized nearly 200 papers from 2015. For a patient, ECG signal analysis can be done by a well-trained DNN model in a fraction of a second, and the result can be very accurate if the training dataset is sufficiently large. It seems that artificial intelligence (AI) doctors are technically ready to serve the patients for ECG diagnosis.

However, DNNs are known to be vulnerable to adversarial noises in the field of computer vision [7]. Adversarial noises are small perturbations to the input of a DNN model, even imperceptible to human eyes, and can significantly change the DNN output. Adversarial noises can be generated by adversarial attack algorithms in two categories: white-box or black-box attacks. It is a white-box adversarial attack if the attacker

\* Corresponding author. Department of Computer Science, University of Miami, Coral Gables, FL, 33146, USA.  
E-mail address: [liang@cs.miami.edu](mailto:liang@cs.miami.edu) (L. Liang).

knows the inner structure of the DNN. Two well-known white-box attacks are Fast Gradient Signed Method (FGSM) [8] and Projected Gradient Descent (PGD) [9]. It is a black-box attack if the attacker has no knowledge of the inner structure of the DNN and can only query the DNN to get the outputs. The typical approach for black-box attacks is transfer-based, in which a substitute DNN model is trained on the input-output pairs of the target DNN model (called oracle) to be attacked, so that the substitute model can learn the decision boundary of the oracle; after training, the substitute is used to construct adversarial noises to attack the oracle [10]. Another approach for black-box attacks is using stochastic sampling methods to estimate the gradient of the target network, and then the estimated gradient can be used for attacks [11]. The weaknesses of black-box attacks are studied by Jonathan Uesato et al. in Ref. [11], which shows that compared to white-box attack, black-box attacks are less likely to succeed and may have much higher computation costs. From the perspective of the defender, in this study, we consider the worst-case scenario that the attacker knows the DNN structure (i.e., white-box attacks). Adversarial attacks pose significant threats [7] to DNN-based systems for life-critical applications, e.g., vision-based self-driving. A recent study shows that adversarial noises can also cause DNNs to make wrong classifications of ECG signals [12]. Adversarial noises can be added by an attacker to an ECG signal after it is recorded from a patient and before it is processed by a DNN classifier. By doing so, the attacker may achieve personal gains at the expense of the patient.

Little effort has been devoted to solving the robustness issue in ECG applications. The robustness issue is unfortunately neglected by the US Food & Drugs Administration (FDA): some AI/DNN algorithms for ECG analysis [13] have already been FDA-cleared/approved, making impacts on human lives. For the best interest of the consumers/patients, it is urgently needed to develop methods to improve DNN robustness against adversarial noises.

As a comparison, lots of effort has been made to develop defense methods in the field of computer vision [11,14,15], to improve DNN robustness against adversarial noises for image classification applications. Currently, the most popular and effective defense strategy is adversarial training, and the basic idea is to generate adversarial noises through an adversarial attack, add the noises to the images, and then use both the clean images (without adversarial noises) and the noisy images (added with adversarial noises) for training a DNN model. A noisy image is called an adversarial sample. Through adversarial training, a DNN model may be able to recognize adversarial samples and therefore become robust to adversarial noises. Different adversarial training-based defense methods have been proposed [7,14–16], which share the same basic idea and vary in how the adversarial samples are generated. Adversarial training is straightforward but has problems. For example, it is very computationally expensive and time-consuming to generate adversarial samples, and very-noisy adversarial samples can be misleading and reduce the classification accuracy of the DNNs. Parallel to adversarial training, regularization terms can be added to the loss function during model training to reduce the sensitivity of the model output with respect to the input. Regularization terms could be the gradient magnitude of the loss [17] or Jacobian regularization [18], which has good performance for image classification applications. It is unknown whether these defense methods designed for image classification applications work for ECG classification applications.

In this study, we propose a novel regularization method to minimize the Noise-to-Signal Ratio (NSR) during the training process to improve DNN robustness against adversarial noises for ECG classification applications. We used the PGD algorithm [9] to implement white-box adversarial attacks, which is widely used for robustness evaluation [15]. In addition, we also used Smooth Adversarial Perturbations (SAP) algorithm [12] for adversarial attacks. We evaluated the proposed method on two public datasets: PhysioNet MIT-BIH Arrhythmia ECG (MIT-BIH) dataset [19] and China Physiological Signal Challenge 2018 (CPSC2018) [20,21] dataset, and the results show that our proposed

method leads to an enhancement in robustness against the adversarial attacks, with a minimal reduction in accuracy on clean data. The code of our method is publicly available.

The Novelty of the paper: Our preliminary study was presented at conferences [22,23], which, to our best knowledge, is the first work to improve DNN robustness against adversarial noises for ECG signal classification. In this paper, we present our complete study, including (1) detailed explanation of our method, (2) comparison with other methods using fine-tuned parameters, (3) defense against PGD, SAP, and white-noise attacks, and (4) extensive evaluation on two datasets.

Before diving into the details of the method, we would like to show the severity of the issue by an example in Fig. 1. Given an ECG signal  $x$  (we call it clean signal although it may have some noises during the ECG recording process) as input, a DNN model will predict the class label of the signal. The true class label is "N", and the prediction from the model is correct for the input  $x$  (Fig. 1(a)). A noisy signal  $x_e = x + \delta$  is obtained (Fig. 1(b)) by adding a small amount of adversarial noise  $\delta$  to  $x$  through an adversarial attack. Given  $x_e$  as input, the DNN model outputs the class label "V". The noise amplitude is so small that it is hardly detectable by the human eyes, but the DNN model thinks that  $x$  and  $x_e$  are completely different and therefore assigns different class labels to  $x$  and  $x_e$ . Would you trust an AI-based ECG-analysis system if it may make such "unbelievable" mistakes?

## 2. Methodology

### 2.1. The proposed method using NSR regularization

Our method has a new loss function to improve DNN robustness by reducing Noise-to-Signal Ratio (NSR). The noise refers to the adversarial noise generated from an adversarial attack. The signal refers to the output of the DNN classifier (i.e., the logits before the softmax layer). Our method assumes that the nonlinear activation function is ReLU or its variants (e.g., LeakyReLU), and the DNN may have the standard layers, including convolution layers, fully connected layers, pooling layers, batch-normalization layers, dropout layers, and skip-connections. The idea of our method is to apply regularization during model training in order to minimize NSR. Given an input sample/signal  $x$  (reshaped to a vector), the output of a DNN can be exactly expressed by a linear equation [24,38–40]:

$$z = W^T x + b \quad (1)$$

where the weight matrix  $W$  is an implicit function of  $x$ , and the bias vector  $b$  is also an implicit function of  $x$ . Thus, the DNN is a piecewise linear function on the input space. The output of the DNN is a vector  $z = [z_1, \dots, z_K]^T$ , where  $z_i$  is the output logit of class- $i$  and the total number of classes is  $K$ . Let  $w_i$  be the  $i$ -th column of  $W$  and  $b_i$  be the  $i$ -th element of  $b$ . Let  $y$  be the true label of  $x$ . Then we have:

$$z_y = w_y^T x + b_y \quad (2)$$

During an adversarial attack, a noisy vector  $\delta$  is generated and added to the input  $x$ , and then the new output is:

$$z_{y,\delta} = w_{y,\delta}^T (x + \delta) + b_{y,\delta} \quad (3)$$

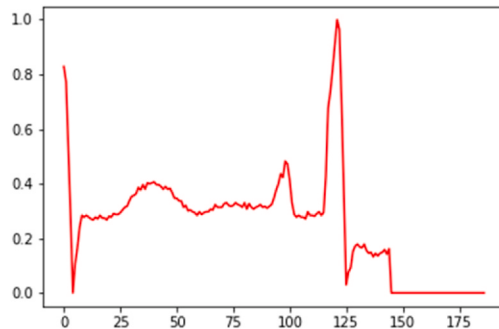
By definition [25], adversarial noise has small amplitude but may lead to the change of DNN output. When the amplitude of the noise  $\delta$  is small enough, then  $w_y \approx w_{y,\delta}$  and  $b_y \approx b_{y,\delta}$ . Therefore, we obtain:

$$z_{y,\delta} \approx w_y^T x + b_y + w_y^T \delta = z_y + w_y^T \delta \quad (4)$$

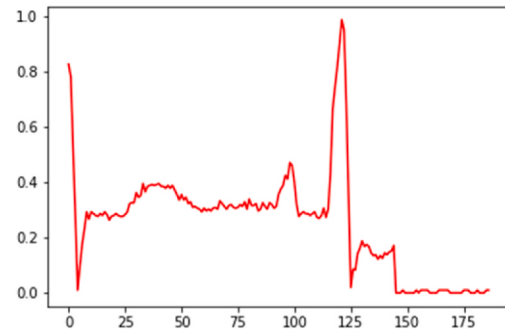
We define NSR and apply Hölder's inequality:

$$\text{NSR}_y = \frac{|w_y^T \delta|}{|z_y|} \leq \frac{\|w_y\|_q \cdot \|\delta\|_p}{|z_y|} \quad (5)$$

where  $\frac{1}{p} + \frac{1}{q} = 1$ . In this work, we focus on L-infinity norm  $\|\delta\|_\infty = \varepsilon_\delta$ ,



(a) clean ECG, classified as "N"



(b) ECG on noise level 0.01, classified as "V"

Fig. 1. MIT-BIT data sample with no noise (a) and small adversarial noise (b).

and therefore:

$$NSR_y \leq \frac{\|w_y\|_1 \cdot \varepsilon_\delta}{|z_y|} = R \quad (6)$$

By combining the regularization term  $R$  with Mean Square Error (MSE) loss and margin loss for classification, the complete loss function for training a robust DNN model is obtained:

$$L_{NSR} = (z_y - 1)^2 + \sum_{i \neq y} (z_i - 0)^2 + \sum_{i \neq y} \max(0, 1 - z_y + z_i) + \beta \log(R + 1) \quad (7)$$

In the experiment,  $\varepsilon_\delta$  is set to 1 because the maximum signal amplitude is 1, and  $\beta$  is determined on the validation set. The margin loss  $\sum_{i \neq y} \max(0, 1 - z_y + z_i)$  and the regularization term  $\log(R + 1)$  are only used for correctly classified samples; and for wrongly classified samples,  $L_{NSR}$  only contains the MSE loss. For the experiment on the CPSC2018 dataset, to facilitate the convergence during the training process, the regularization term and the margin loss will not be added to the loss function until the 11-th epoch.

In this paper, two metrics are used to measure the performance of a DNN classifier: classification accuracy averaged across all classes, which will be simply called “accuracy”, and F1 score averaged across all classes, which will be simply called “F1”.

To use the NSR Regularization-based new loss function defined by Eq. (7), a proper  $\beta$  is needed to achieve a good balance between robustness and accuracy. For this purpose, we define a new metric to measure the overall performance of a classifier, which is given by:

$$ACC_{robust} = \sqrt{ACC_{clean} \times AUC_{\|\delta\|_\infty \leq \varepsilon_{max}}} \quad (8)$$

Here,  $ACC_{clean}$  is the accuracy on clean data (without adversarial noises).  $AUC_{\|\delta\|_\infty \leq \varepsilon_{max}}$  is the normalized area under the curve of accuracy vs. noise level, which is the accuracy averaged across a range of noise levels, i.e.,  $\|\delta\|_\infty \leq \varepsilon_{max}$ . Therefore,  $ACC_{robust}$  is the overall performance measure that takes both clean accuracy (i.e., accuracy on clean data) and robustness (i.e., accuracy on noisy data) into consideration, and a better  $\beta$  should lead to a higher  $ACC_{robust}$ . By definition [25], adversarial noise is small change in the input, which may result in a large change in the output of a DNN. Thus, we only consider the noises within a certain range, i.e., setting a maximum noise level  $\varepsilon_{max}$  for method evaluation. When the noise amplitude is large enough, the content/meaning of the input signal  $x + \delta$  is significantly altered, and the output of the model is expected to change. In the experiment, the  $\varepsilon_{max}$  of  $ACC_{robust}$  for the MIT-BIT dataset is 0.1 and the  $\varepsilon_{max}$  of  $ACC_{robust}$  for the CPSC2018 dataset is 0.01, and the explanation is in Section 3. Another metric  $F1_{robust}$  is defined in the same way, and its formula is in Appendix B.

## 2.2. PGD-based adversarial attack and adversarial training

For method evaluation, we used the algorithm, named Projected Gradient Descent (PGD), to implement the adversarial attack [9], which is regarded as the strongest first-order white box adversarial attack and is widely used for robustness evaluation [11,15]. For the convenience of the reader, we provide a summary of the PGD-based adversarial attack. The key equation of the PGD attack is given by:

$$x^k = \prod (x^{k-1} + \alpha \cdot sign(\nabla_x J(x^{k-1}))) \quad (9)$$

where  $\alpha$  is the step size and  $x^k$  is the adversarial example from the  $k$ -th iteration. The adversarial noise after the  $k$ -th iteration is  $\delta = x^k - x$ . If the magnitude of the noise  $\delta$  is larger than the given noise level  $\varepsilon$  for the attack, the projection operation  $\prod()$  will project it back onto a  $\varepsilon$ -ball, i.e.,  $\|x^k - x\|_\infty \leq \varepsilon$ . Assuming  $x$  is correctly classified by a DNN classifier, then, after a total number of  $K$  iterations, the objective  $J$  of the attack on the noisy sample  $x^k$  becomes very large such that  $x^k$  is wrongly classified. Usually, the objective  $J$  is the cross-entropy function that is high when classification accuracy is low. Therefore, the attack can be summarized by a single function:  $x_\varepsilon = PGD(x, y, \varepsilon, \alpha, K)$ , where  $x_\varepsilon = x^K$  is the generated adversarial sample on the noise level  $\varepsilon$ . The default value of the step size  $\alpha$  is 0.01 [9]. The attack strength is determined by  $K$ , the number of iterations. A PGD attack with  $K$  iterations is known as K-PGD, and the strong 100-PGD is usually used for robustness evaluation [11, 15]. By varying the noise level  $\varepsilon$  of the 100-PGD attack, the robustness of a DNN model can be evaluated by measuring its accuracy on the adversarial samples in a large range of noise levels.

The basic idea of adversarial training [8] is to generate adversarial samples by an algorithm (e.g., PGD) and use the adversarial samples as part of the training data. In this way, the trained model may become robust against adversarial noises. The loss function of the standard adversarial training [8] is given by:

$$L_{adv} = 0.5L_{CE}(x, y) + 0.5L_{CE}(x_\varepsilon, y) \quad (10)$$

where  $L_{CE}$  is the standard cross-entropy loss and  $x_\varepsilon$  is an adversarial sample (e.g., generated by PGD) on the noise level  $\varepsilon$ . As shown in Section 3, the performance of PGD-based adversarial training is determined by the noise level  $\varepsilon$ . To choose a proper value of  $\varepsilon$ , we tried a series of experiments with different values of  $\varepsilon$ , and chose the best one associated with the highest  $ACC_{robust}$  (Eq. (8)) on the validation set.

The standard adversarial training encountered a convergence problem on the CPSC2018 dataset. To help convergence, the adversarial loss  $L_{CE}(x_\varepsilon, y)$  will not be used until the 11-th epoch, and the level of noise is scaling up linearly as the number of epochs increases during training [24]:

$$\varepsilon_t = \varepsilon(t - 10) / (t_{max} - 10) \quad (11)$$

where  $t$  is the index of the training epoch,  $t_{max}$  is the total number of training epochs, and  $\epsilon_t$  is the level of noise added to the clean samples during the current epoch  $t$ .

### 2.3. The Jacobian Regularization based method

For method comparison, we implemented the Jacobian Regularization based method [18] which was designed for image classification applications. The basic idea of the method is to penalize the large gradient of the output with respect to the input, which makes the DNN model less sensitive to the change in the input. The sensitivity to input change is measured by the Frobenius norm of the DNN's Jacobian matrix, which can be added to the loss function as a regularization term. The loss function of the method is given by:

$$L_{jacob} = \sum_{n=1}^N L_{CE}(x_n, y_n) + \lambda \sqrt{\sum_{d=1}^D \sum_{k=1}^K \sum_{n=1}^N \left( \frac{\partial}{\partial x_d} z_k(x_n) \right)^2} \quad (12a)$$

Here,  $L_{CE}$  is the standard cross-entropy loss.  $D$  is the input dimension.  $K$  is the number of classes.  $N$  is the batch size during training.  $\{x_1, x_2, \dots, x_i, \dots, x_N\}$  are the samples/signals in a mini-batch, and  $n$  is sample index in the mini-batch.  $y_n$  is the ground truth label of  $x_n$ .  $z = [z_1, \dots, z_K]^T$  is the output logits of the DNN, and  $z_k(x_n)$  is a logit of the input sample  $x_n$ .  $x_d$  refers to the  $d$ -th dimension of a sample  $x_n$ .

The original loss function in Eq. (12a) caused a numerical problem when it was applied for the high dimension data in the CPSC2018 dataset. Thus, we slightly modified the loss function in our experiment, which is given by:

$$L_{jacob} = \frac{1}{N} \sum_{n=1}^N L_{CE}(x_n, y_n) + \frac{\lambda}{NK} \sqrt{\sum_{d=1}^D \sum_{k=1}^K \sum_{n=1}^N \left( \frac{\partial}{\partial x_d} z_k(x_n) \right)^2} \quad (12b)$$

To further improve convergence, the regularization term will not be added to the loss function until the 11-th epoch during training on the CPSC2018 dataset.

### 2.4. The customized DNNs

We tested two DNNs on the MIT-BIH dataset: a 1-D CNN and an MLP. The CNN is borrowed from a previous work by Kachuee et al. in Ref. [26], which has 30 layers in total and achieved excellent classification performance. The MLP is designed by us as a baseline model, and it has 8 layers. The MLP structure is (187-128)-RELU-(128-128)-RELU-(128-128)-RELU-(128-32)-(32-5). We refer the reader to our source code for more details of the two models.

For the CPSC2018 dataset, we designed a 1-D CNN to classify the ECG signals and handle the challenge caused by variable signal length. The high-level architecture of this CNN is shown in Fig. 2. To describe the CNN, we use "Cov (a, b, c, d, e)" to represent a convolution layer with "a" input channels, "b" output channels, kernel size of "c", stride of "d" and padding of "e"; "Linear (f, g)" to denote a linear layer with input size of "f" and output size of "g"; "MaxPool (h, i, j)" to denote max-pooling with kernel size of h, stride of i and padding size of j; "AvgPool (k, l, m)" to denote average-pooling with kernel size of k, stride of 1 and padding size of m; "GN" to denote group normalization [27]. The network has 4 convolution blocks of the same structure, which will shrink the size of the input tensor and double the number of channels. To handle a time sequence with variable length, RNN is typically used. However, it is known that RNN runs very slow due to the difficulty of parallel computing. To enable the CNN to handle variable signal length, we used zero-padding and input/output-masking. Each signal (i.e., the ECG recording from a patient) is padded with zeros to a fixed length of 33792, so that the padded signals can be assembled into mini-batches for parallel computing. An input mask with a fixed length of 33792 is used by the CNN to ignore the zeros in each padded signal. For valid elements

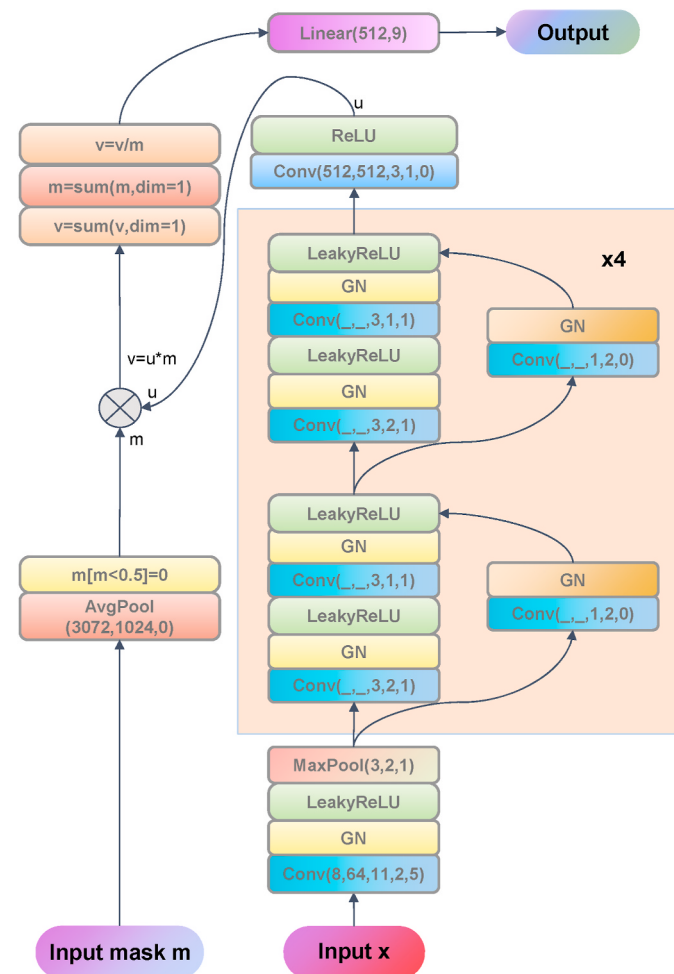


**Fig. 2.** The high-level architecture of the CNN. The size of the input mask is the same as the size of the input  $x$ . The mask will help the network ignore the padded zero elements in  $x$ , which has a variable length. The network outputs the classification scores (a.k.a. logits).

of a padded signal, the corresponding elements of its mask are ones. For zero elements of a padded signal, the corresponding elements of its mask are zeros. To obtain the output mask, an average-pooling is applied to the input mask. Then, a valid output vector is obtained by multiplying the output mask and the feature output from the last convolution block. After this output-masking operation, a channel-wise averaging weighted by the mask is performed to reduce the dimension of the output vector from a variable length to a fixed length of 512. The fixed length output is then processed by the final linear layer to obtain the classification scores (a.k.a. logits). We refer the reader to the source code for more details of the CNN model.

## 3. Experimental evaluation of the methods

### 3.1. Datasets

We used the processed MIT-BIH dataset from a previous study [26, 28], which used the annotations in the original MIT-BIH dataset to create five different beat categories in accordance with the Association for the Advancement of Medical Instrumentation (AAMI) EC57 standard [29]. The original MIT-BIH dataset consists of ECG recordings at the sampling rate of 360 Hz, which involves 47 subjects: 25 men aged between 32 and 89, and 22 women aged between 23 and 89. The recordings were independently labeled beat-by-beat by two or more cardiologists. The processed dataset contains individual heartbeats that

have been segmented from the recordings, and subsequently resampled and zero-padded. The ECG signal of one heartbeat is a 1D array of 187 numbers, which is referred to as a sample in this study. The task is to predict the class label of a sample from the 5 categories, which are N (Normal, Left/Right bundle branch block, Atrial escape, and Nodal escape), S (Atrial premature, Aberrant atrial premature, Nodal premature and Supra-ventricular premature), V (Premature ventricular contraction and Ventricular escape), F (Fusion of ventricular and normal) and Q (Paced, Fusion of paced and normal and Unclassifiable). The processed dataset has been divided into a training set (87554 samples) and a test set (21892 samples) in the previous study [26], which is publicly available at [28]. We note that a different train-test split may lead to a different accuracy, which makes it difficult to directly compare the ECG classification methods in the literature [4]. By using a publicly available dataset with a given train-test split, the results in this study can be used for direct comparison with new defense methods that may be developed in the future. To handle class imbalance, we performed up-sampling to ensure that there is equal number of samples in the classes in the training set and the test set, i.e., the five classes are equally important. We further divided the training set into a “pure” training set (70043 samples, 80%) and a validation set (17511 samples, 20%) that was used to find the best parameters of the methods.

The other dataset, CPSC2018 is described in detail by Ref. [21]. There are 6877 ECG 12-lead recordings in this dataset. The ECG signals were sampled by the frequency of 500 Hz, and the duration is in the range of 6–60 s (note: a few signals have 144 s). Namely, each ECG sample (i.e., the whole digit ECG signal from a patient) in the dataset has 12 leads/channels, and each sample has a variable length (i.e., time-points) from 3000 to 72000. This dataset has 9 categories, which are “Normal” (918 samples), “Atrial Fibrillation (AF)” (1098 samples), “First-Degree Atrioventricular Block (I-AVB)” (704 samples), “Left Bundle Branch Block (LBBB)” (207 samples), “Right Bundle Branch Block (RBBB)” (1695 samples), “Premature Atrial Contraction (PAC)” (556 samples), “Premature Ventricular Contraction (PVC)” (672 samples), “ST-segment Depression (STD)” (825 samples) and “ST-segment Elevated (STE)” (202 samples). There are only class labels on the recording level, and beat-by-beat labels are not available, unlike the MIT-BIH dataset that has been labeled beat-by-beat. And therefore, the task is to predict the class label of a recording from a patient. We pre-processed the data according to the examples provided by the CPSC2018 committee. First, we removed the samples with multiple labels (477 samples). Second, from each class, we randomly put 5 samples into the validation set and 50 samples into the test set. In this way, we split the dataset into a training set of 5905 samples, a validation set of 45 samples, and a test set of 450 samples. Because this dataset is class-imbalanced, upsampling was done to ensure that the training set is class-balanced. Third, for each sample, we removed Lead 3, 4, 5 and 6, due to the fact that Lead 3, 4, 5 and 6 are redundant and can be derived from the other leads [31]. Fourth, for each sample, we scaled each lead by its maximum absolute value so that the magnitude of each lead is within the range of -1 to 1 [32], which is the standard way to do feature normalization. Then, we randomly padded each sample with 0 on both ends during training, such that the temporal length of a padded single is 33792. For a few samples with a length larger than 33792, we discarded the signal elements after 33792. As a result, each sample after pre-processing is a tensor with the shape of  $8 \times 33792$ . Randomly padding 0 on both ends of a signal is data augmentation to shift a single to left or right along the time axis. We have made the preprocessing method publicly available (see the link at the end of the paper).

### 3.2. Model training and parameter tuning

The metric in Eq. (8) is used for parameter tuning. In this study, we set  $\epsilon_{max} = 0.1$  for the MIT-BIH dataset and  $\epsilon_{max} = 0.01$  for the CPSC2018 dataset. On the MIT-BIH dataset, when the noise level of the PGD attack is higher than 0.1, the generated adversarial samples/signals become

very noisy and hardly recognizable by the human eye. On the CPSC2018 dataset, when the noise level is higher than 0.01, the noises in the signals become noticeable by the human eye, and the performance of the methods starts to drop quickly.

Given a dataset and a DNN structure, tuning the parameter of a method is to train DNN models with different parameter values on the training set, and measure the performance of each trained model on the validation set. The parameter associated with the best performed model is the best parameter. For clarity, we give different names to the DNN models trained by the three defense methods. The model (MLP or CNN) trained by our new loss  $L_{NSR}$  is named “ $\beta$  NSR” where  $\beta$  is the parameter. The model trained by the loss  $L_{Jacob}$  is named “ $\lambda$  Jacob” where  $\lambda$  is the parameter. The model trained by the loss  $L_{adv}$  is named “adv  $\epsilon$ ” where  $\epsilon$  is the noise level for PGD-based adversarial training. In addition, we trained models with the standard cross entropy loss, and the name of each trained model is “CE”.

For the experiment on the MIT-BIH dataset, the models were trained for 50 epochs with batch size of 128. The Adamax optimizer was used with the learning rate of 0.001. For the experiment on the CPSC2018 dataset, the models were trained for 70 epochs with batch size of 64. The Adam optimizer was used with the learning rate of 0.001. The selection of optimizers and learning rates was done by a grid search, as shown by Table 7 (A-C) in Appendix A.

The experiment was conducted on a server with Nvidia Tesla V100 GPU (32 GB memory) and Intel(R) Xeon(R) E5-2698 v4 CPU (2.20 GHz). The operating system is CentOS 7. Python version is 3.8.3, and Pytorch version is 1.5.0. On the CPSC2018 dataset, it took about 2 h to train a “CE” model, 12 h to train a “ $\beta$  NSR” model, 24 h to train a “ $\lambda$  Jacob” model, and 12 h to train an “adv  $\epsilon$ ” model. On the BIT-MIT dataset, for the CNN, it took about 1.28 h to train a “CE” model, 8.89 h to train a “ $\beta$  NSR” model, 8.61 h to train a “ $\lambda$  Jacob” model, and 9.17 h to train an “adv  $\epsilon$ ” model. On the BIT-MIT dataset, for the MLP, it took about 0.36 h to train a “CE” model, 1.81 h to train a “ $\beta$  NSR” model, 1.15 h to train a “ $\lambda$  Jacob” model, and 1.31 h to train an “adv  $\epsilon$ ” model.

For our method, we varied the parameter  $\beta$  in the range of 0.1–1.0 for the MIT-BIH dataset and in the range of 0.4–1.2 for the CPSC2018 dataset, which resulted in a large variation of model performance. The results are reported in Table 1 (A to C) in Appendix A, which show the accuracy of each “ $\beta$  NSR” model (MLP or CNN) on validation set under the 100-PGD attack. Clean data has the noise level of 0. The best  $\beta$  is 0.4 for the MLP on the MIT-BIH dataset with  $ACC_{robust} = 0.854$ . The best  $\beta$  is 0.3 for the CNN on the MIT-BIH dataset with  $ACC_{robust} = 0.894$ . The best  $\beta$  is 1.0 for the CNN on the CPSC2018 dataset with  $ACC_{robust} = 0.889$ .

For the Jacobian Regularization based method, we varied the parameter  $\lambda$  in a large range, which resulted in a large variation of model performance. The results are reported in Table 2 (A to C) in Appendix A, which show the accuracy of each “ $\lambda$  Jacob” model on validation set under the 100-PGD attack. Clean data has the noise level of 0. The best  $\lambda$  is 0.9 for the MLP on the MIT-BIH dataset with  $ACC_{robust} = 0.770$ . The best  $\lambda$  is 0.7 for the CNN on the MIT-BIH dataset with  $ACC_{robust} = 0.806$ . The best  $\lambda$  is 24.0 for the CNN on the CPSC2018 dataset with  $ACC_{robust} = 0.836$ .

For the adversarial training method, we varied the parameter  $\epsilon$  in the range of 0.05–0.3 for the MIT-BIH dataset and 0.005 to 0.1 for the CPSC2018 dataset, which resulted in a large variation of model performance. The results are reported in Table 3 (A to C) in Appendix A, which show the accuracy of each “adv  $\epsilon$ ” model on validation set under the 100-PGD attack. Clean data has the noise level of 0. The best  $\epsilon$  is 0.1 for the MLP on the MIT-BIH dataset with  $ACC_{robust} = 0.799$ . The best  $\epsilon$  is 0.1 for the CNN on the MIT-BIH dataset with  $ACC_{robust} = 0.863$ . The best  $\epsilon$  is 0.01 for the CNN on the CPSC2018 dataset with  $ACC_{robust} = 0.796$ . We used 10-PGD for adversarial training on the MIT-BIH dataset, and 20-PGD for adversarial training on the CPSC2018 dataset, which are weaker than 100-PGD used for method evaluation. We did not use 100-PGD for adversarial training because: (1) it would be cheating to use the

same settings for adversarial training and evaluation; and (2) it will take 60 h to complete the training of a model with a given parameter, and therefore it will take 660 h (27.5 days, non-stop) to complete the experiments for finding the best parameter on the CPSC2018 dataset using an Nvidia V100 GPU, and as a result, the total computing cost will exceed our computing budget. Thus, we chose 10-PGD and 20-PGD to keep the computing cost feasible for adversarial training, which is roughly the same as the cost of our method and the cost of the Jacobian Regularization based method.

### 3.3. Evaluation of the methods using the 100-PGD adversarial attack

For each model trained by a method with the optimal parameter on a dataset (MIT-BIH or CPSC2018), the performance of the model on the test set was evaluated by using the 100-PGD attack. To evaluate a

trained model, for each clean sample in the test set, the corresponding adversarial samples on different noise levels were generated by the 100-PGD attack, and the model was applied to classify these adversarial samples to obtain the accuracy scores on different noise levels. Therefore, for a trained model, a curve of accuracy vs. noise level was obtained. Besides accuracy, the F1 Score was also calculated for each trained model. Then,  $F1_{robust}$  and  $ACC_{robust}$  were calculated as the overall performance measures. The evaluation results on the MIT-BIH dataset and the CPSC2018 dataset are visualized by Fig. 3 and reported in Table 4 (A to F) in Appendix A, which show the accuracy and F1 score of the models on the test set under the 100-PGD attack. Examples of the adversarial samples are shown in Fig. 4 and Fig. 5.

Our proposed method achieved the best accuracy and F1 score on all noise levels under the 100-PGD attack to the MLP on the MIT-BIH dataset (Fig. 3(a)&(b)). On the noise level of 0.1, the model “0.4NSR”

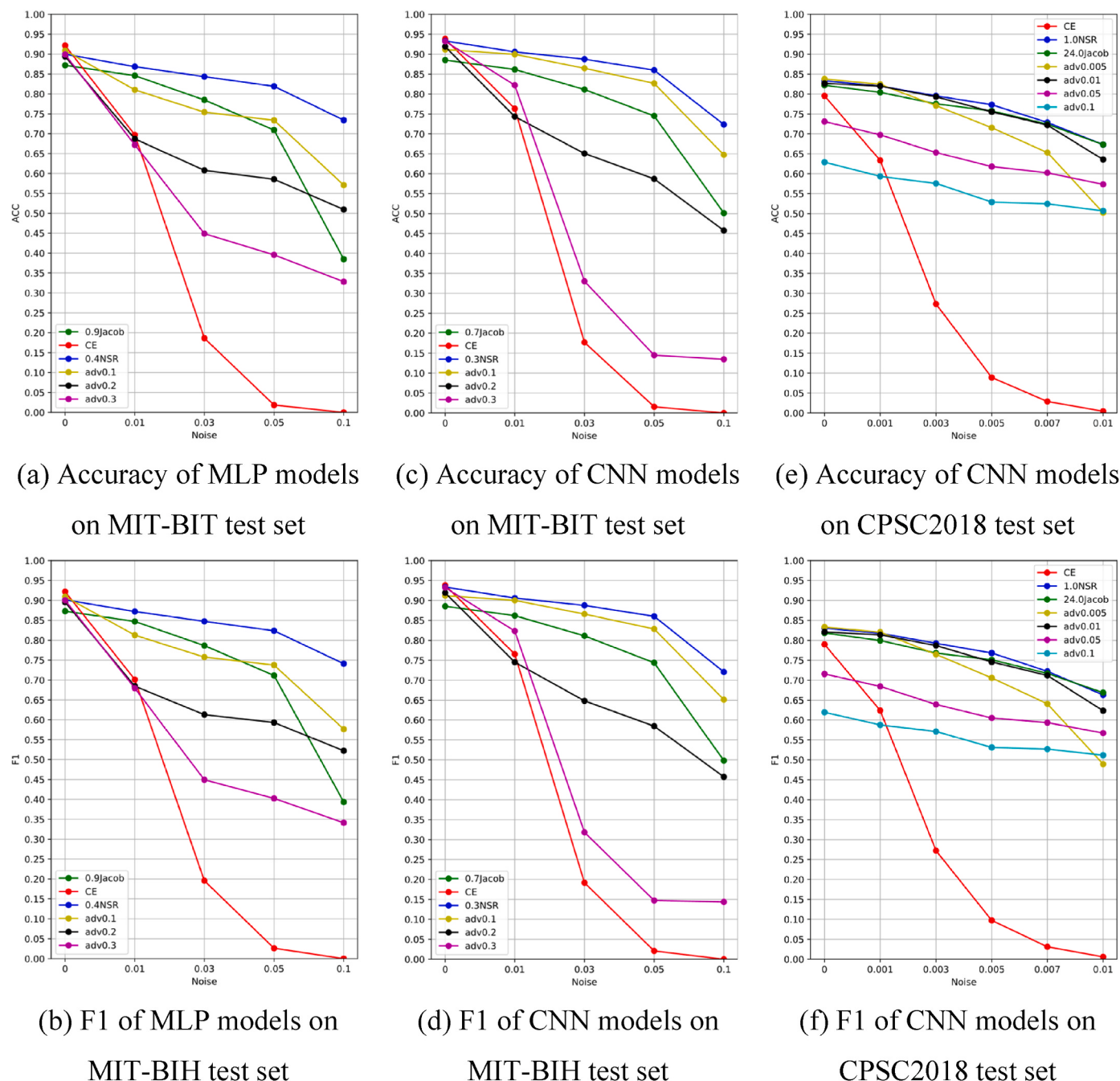
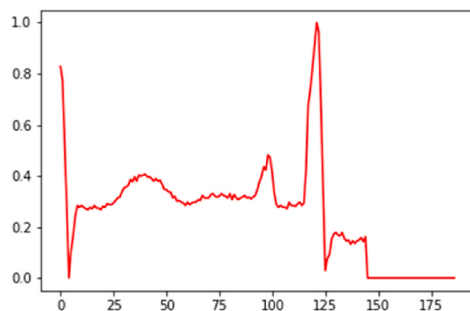
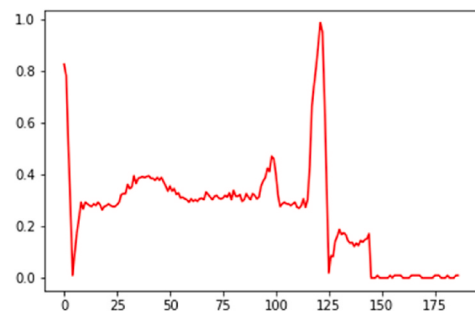


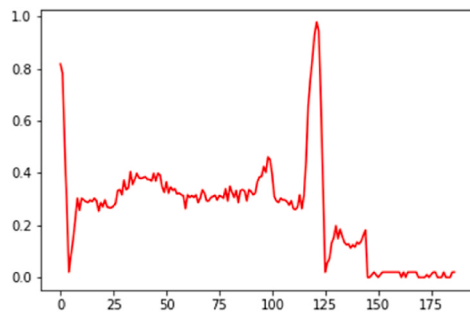
Fig. 3. Evaluation using 100-PGD.



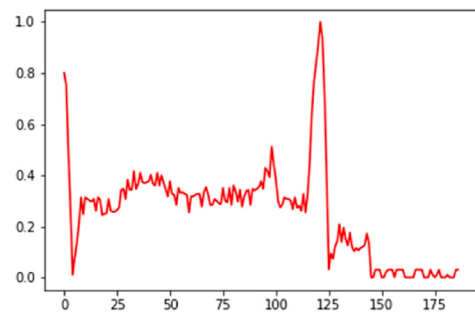
(a) clean ECG (noise level = 0), classified as "N"



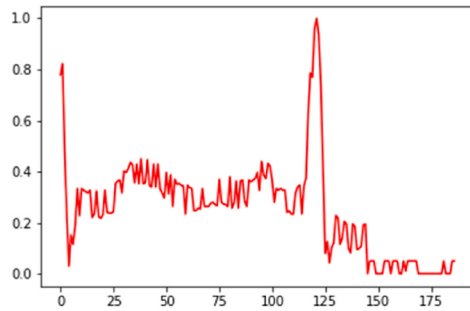
(b) ECG on noise level 0.01, classified as "V"



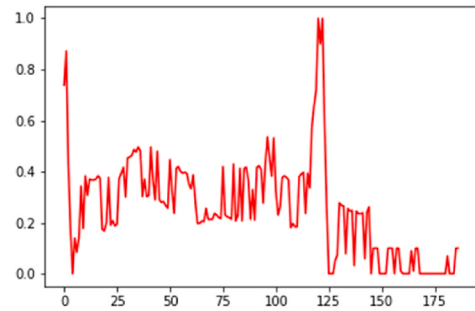
(c) ECG on noise level 0.02, classified as "V"



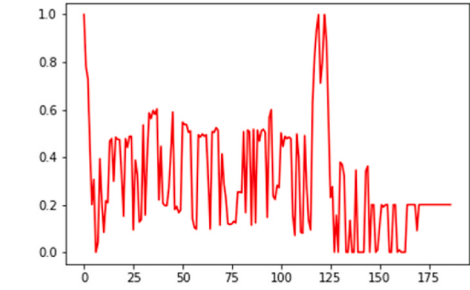
(d) ECG on noise level 0.03, classified as "V"



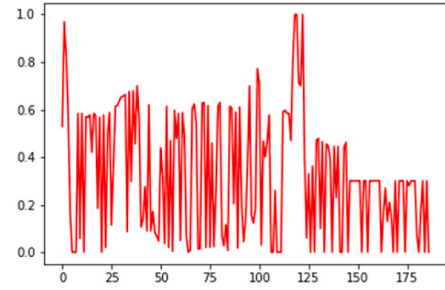
(e) ECG on noise level 0.05, classified as "V"



(f) ECG on noise level 0.1, classified as "V"



(g) ECG on noise level 0.2, classified as "S"



(h) ECG on noise level 0.3, classified as "F"

**Fig. 4.** MIT-BIT ECG signals on different noise levels. The original classification label is N (Normal). However, when the noise level is 0.01, the MLP classified it as V (Premature ventricular contraction and Ventricular escape). The noise is almost not recognizable. Also, when the noise level is larger than 0.1 (Fig. 4 (f)), the original ECG signal is even hardly recognizable by the human eye.

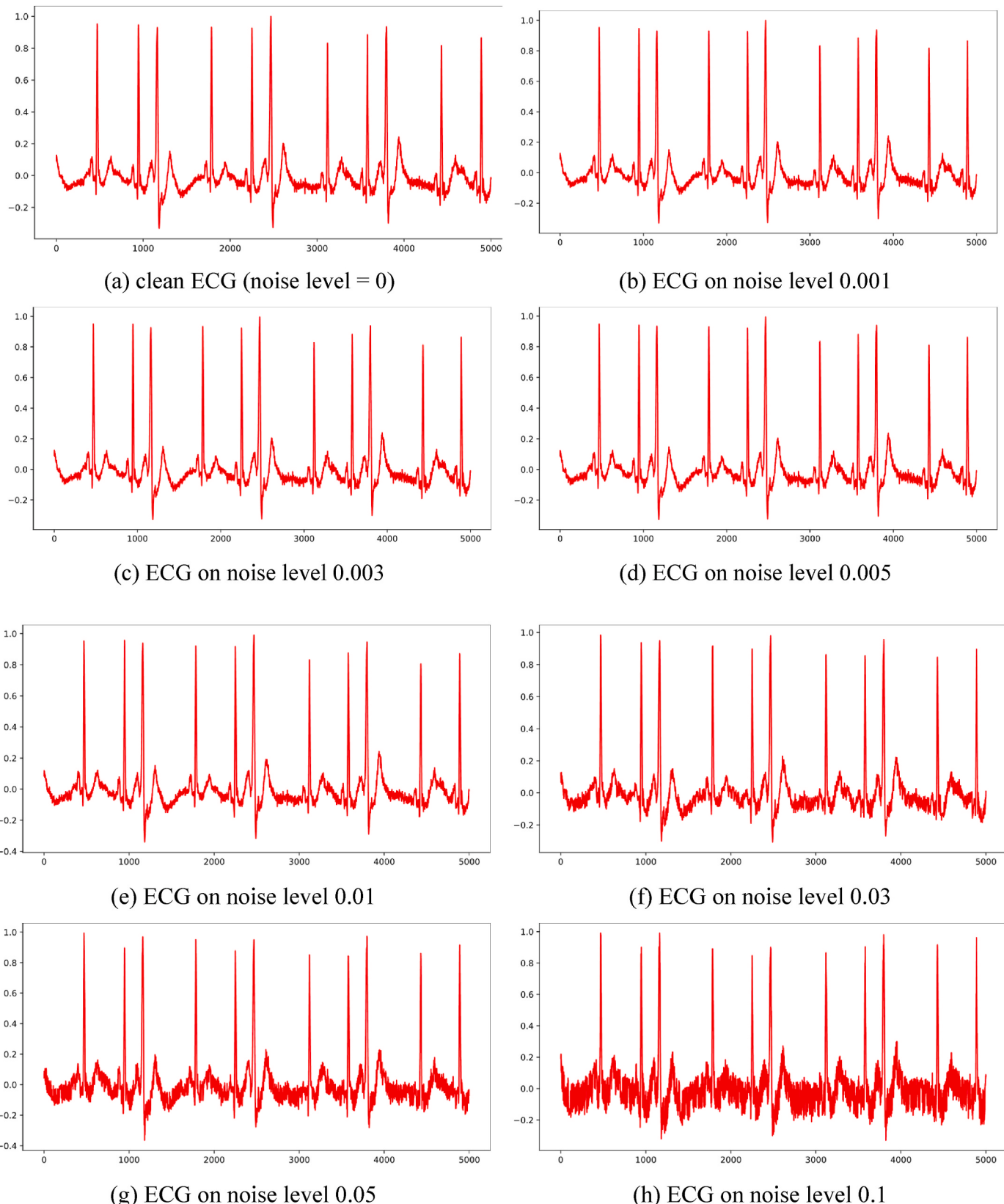


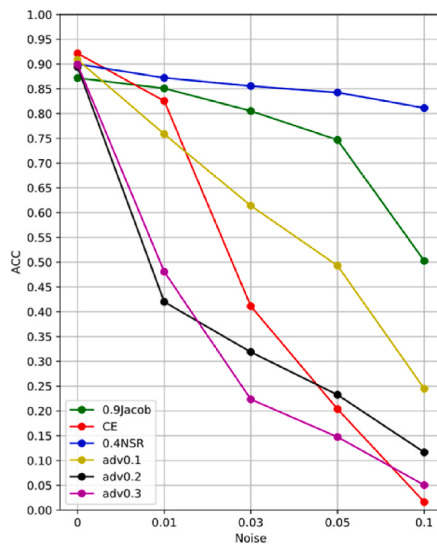
**Fig. 5.** CPSC2018 ECG signal Lead I on different levels of adversarial noises. When the noise level is larger than 0.01 (Fig. 5 (e)), the original ECG signal is even hardly recognizable by the human eye.

has the accuracy of ~75%, which is the highest among the trained models.

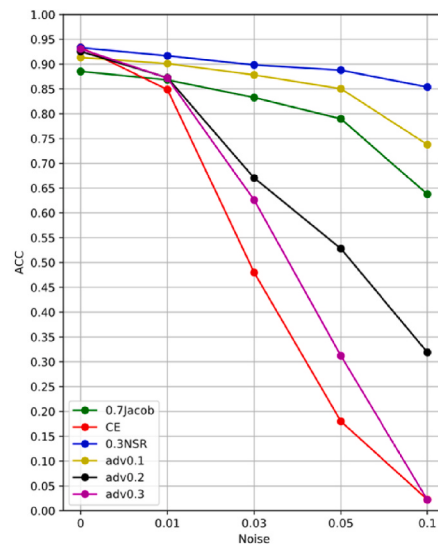
Our proposed method achieved the best accuracy and F1 score when the noise level is within 0.1 under the 100-PGD attack to the CNN on the MIT-BIH dataset (Fig. 3(c)&(d)). On the noise level of 0.1, the model “0.3NSR” can maintain an accuracy of more than 71%. The two models “adv0.2” and “adv0.3” are not as good as the model “0.3NSR” on all of the noise levels, which means these adversarially-trained models are not strong enough to resist against the 100-PGD attack.

Our method performed the best within the noise level of 0.01 under the 100-PGD attack to the CNN on CPSC2018 dataset (Fig. 3(e)&(f)). The 100-PGD attack is so strong that the accuracy of the model “CE” dropped close to 0% on the noise level of 0.01. As a comparison, on the noise level of 0.01, the three models, “1.0NSR”, “24.0Jacob” and

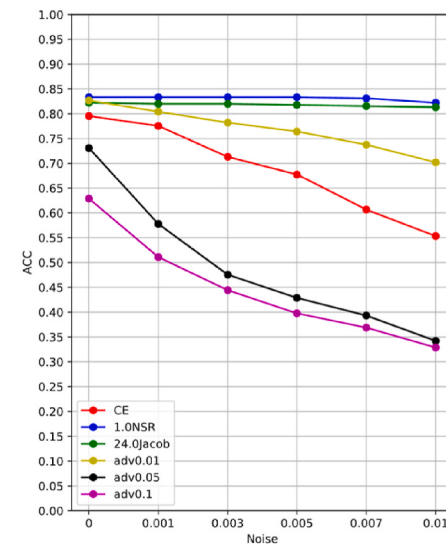
“adv0.01” kept an accuracy of more than 60% and F1 score of more than 0.6. Compared to the model “CE”, the increase in clean accuracy of the model “1.0NSR” is achieved by using the NSR Regularization, and the increase in clean accuracy of the model “adv0.01” is achieved by data augmentation with adversarial samples. This improvement is significant in this challenging task, considering the small sample size (5905 for training) and high input dimension (33792 timepoints per signal). The results suggest that improving robustness may not always be in conflict of increasing accuracy on clean data, as compared to the results on the MIT-BIH dataset. We observed several weaknesses of adversarial training. Each “adv  $\epsilon$ ” model is robust only around the specified noise level of  $\epsilon$ . From Fig. 3(e) and (f), the model “adv0.01” has a good performance on the noise levels of no larger than 0.01, and its accuracy dropped significantly when the noise level exceeds 0.01. Similarly, the



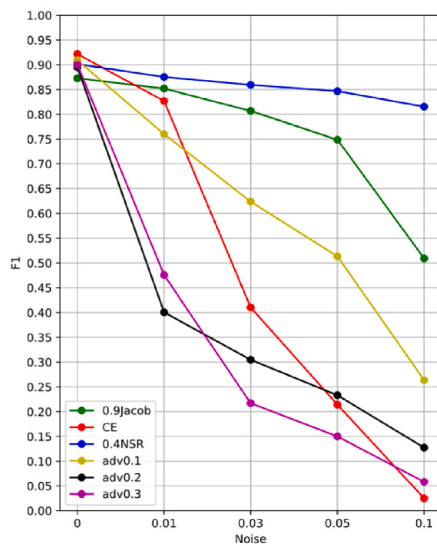
(a) Accuracy of MLP models  
on MIT-BIH test set



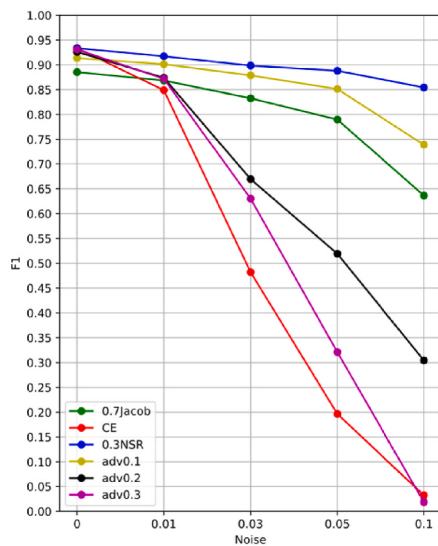
(c) Accuracy of CNN models  
on MIT-BIH test set



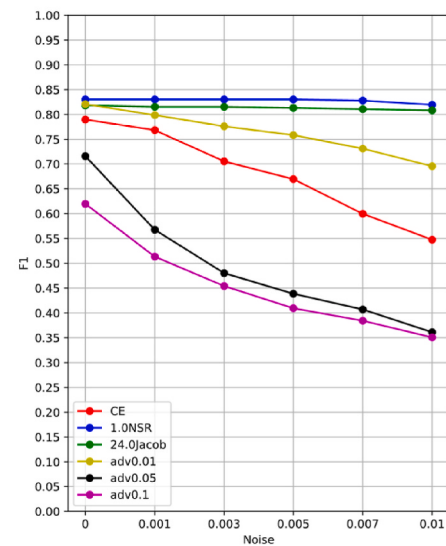
(e) Accuracy of CNN models  
on CPSC2018 test set



(b) F1 of MLP models on  
MIT-BIH test set



(d) F1 of CNN models on  
MIT-BIH test set



(f) F1 of CNN models on  
CPSC2018 test set

Fig. 6. Evaluation using 100-SAP attack.

accuracy of the model “adv0.05” dropped sharply when the noise level exceeds 0.05. A very small noise  $\epsilon$  for adversarial training has almost no effect on CNN robustness (e.g., “adv0.005”). A very large noise  $\epsilon$  for adversarial training led to a significant reduction of accuracy on clean data (e.g., “adv0.05” and “adv0.1”), which can be explained from the preceptive of decision boundary for classification: an adversarial sample on a large noise level may have crossed the optimal decision boundary for classification, and as a result, training with this adversarial sample will lead to a decrease in accuracy on clean data.

We also did an informal comparison with the ECG classification methods reported in the CPSC2018 competition [20]. The model “CE” that was trained only with the standard cross-entropy loss, achieved an accuracy of ~80% and F1 score of ~0.80 on clean data, which would rank in top 6 (F1 scores of the Top-6 methods are 0.837, 0.830, 0.806, 0.802, 0.791 and 0.783). The two models “1.0NSR” and “adv0.01” have

higher accuracy of ~83% and F1 score of ~0.83 on clean data, which would rank in top-3 in the CPSC2018 competition. We note that the top-3 methods in the CPSC2018 competition used recurrent neural networks. Our results show that a similar accuracy on clean data can be achieved by a CNN without recurrent layers.

### 3.4. Evaluation of the methods using the 100-SAP attack

We evaluated the methods using the SAP adversarial attack [12] with different noise levels. The SAP attack was designed specifically to attack ECG signal classifiers by generating smoothed adversarial ECG signals. In this experiment, we used the source code provided by the authors of the SAP attack [12]. The number of iterations in SAP is set to 100, which is similar to the setting of 100-PGD attack. Other parameters of SAP take the default values. The evaluation results are shown in Fig. 6 and Table.

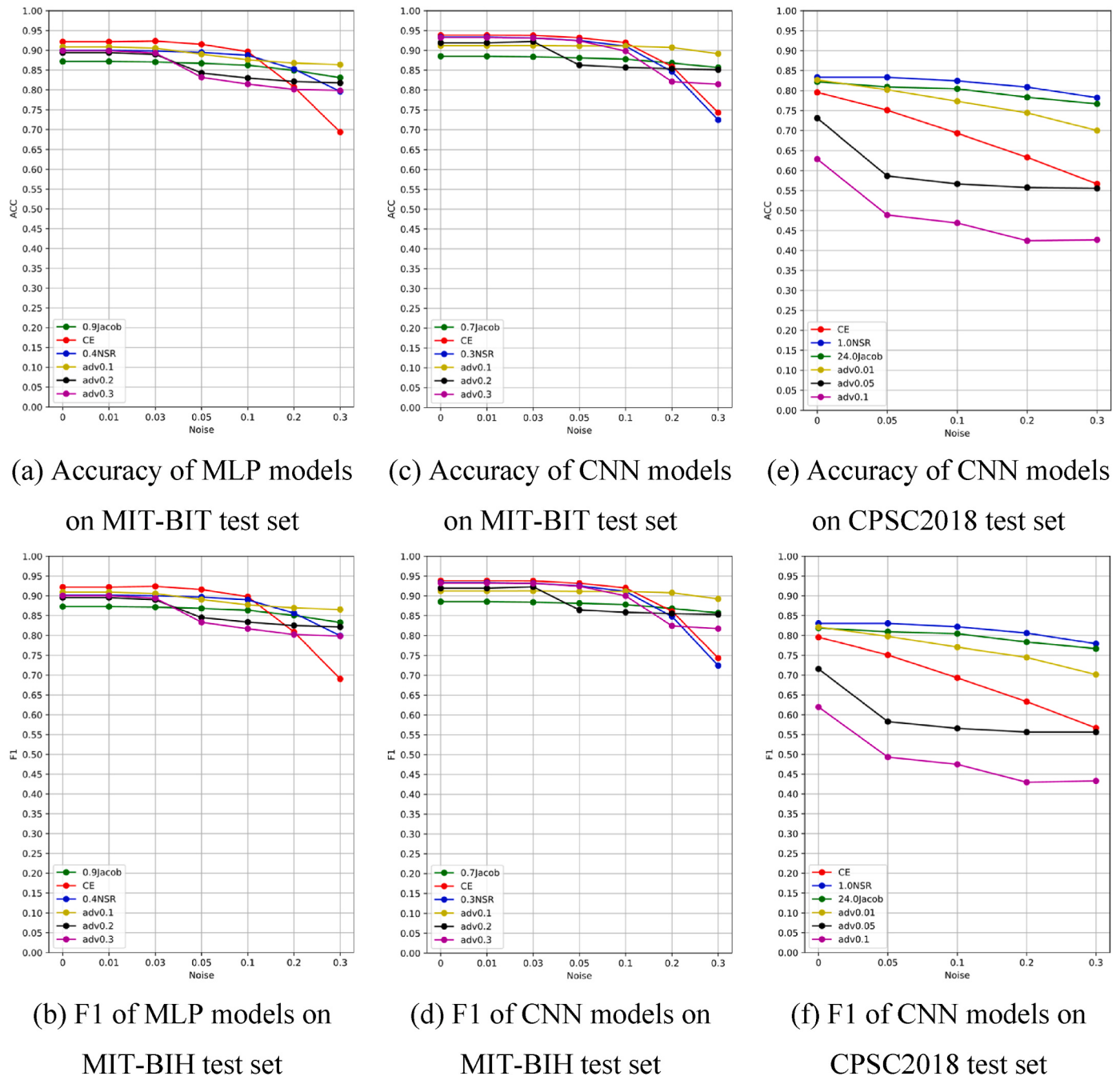


Fig. 7. Evaluation using White-noise Attack.

5 (A to F) in Appendix A, which report the accuracy and F1 of the models on the test set under the 100-SAP attack. Compared to the results of the 100-PGD attack, the 100-SAP attack is much weaker.

Our proposed method achieved the best performance on all noise levels under the 100-SAP attack to the MLP on the MIT-BIH dataset (Fig. 6 (a)&(b)). On the noise level of 0.1, the model “0.4NSR” still held an accuracy of over 80%, but the accuracy of the model “0.9Jacob” dropped close to 50%. All of the “adv  $\epsilon$ ” models had very poor performance.

Our proposed method achieved the best performance on all noise levels under the 100-SAP attack to the CNN on the MIT-BIH dataset (Fig. 6 (c)&(d)). On the noise level of 0.1, the model “0.4NSR” still held an accuracy close to 85%, but the accuracy of the model “0.7Jacob” dropped close to 65%. Among the “adv  $\epsilon$ ” models, only “adv0.1” had comparable performance.

Our proposed method achieved the best performance within the noise level of 0.01 under the 100-SAP attack to the CNN on the CPSC2018 dataset (Fig. 6 (e)&(f)). When the noise level reached 0.01, the models “1.0NSR” and “24.0Jacob” still held an accuracy over 80%. Among the “adv  $\epsilon$ ” models, only “adv0.01” had comparable performance. Compared to the results under the 100-PGD attack, the two models “1.0NSR” and “24.0Jacob” had much better performance, which indicates the 100-SPA attack is much weaker than the 100-PGD attack.

### 3.5. Evaluation of the methods using the white-noise attack

In addition, we tested the performance of each trained model under the white-noises attack, and the results are visualized by Fig. 7 and reported in Table 6 (A to F) in Appendix A, which shows the accuracy and F1 score of the models on the test set under the white noise attack with noise levels in the range of 0–0.3. Basically, white noises from a uniform distribution were added to the samples in the test set, and the accuracy of each trained model on these noisy samples was measured. The maximum amplitude of the white noise is the noise level, and it was varied in a large range. Compared with the 100-PGD attack and the 100-SAP attack, random white noises are more similar to the natural noises in ECG signals, which are originated from ECG recording devices (e.g., electromyogram noise and power line interference).

Under the white-noise attack to the MLP/CNN on the MIT-BIH dataset (Fig. 7 (a)–(d)), the model “CE” trained with the standard cross-entropy performed the best within the noise level of 0.1, which indicates that the standard classifiers naturally have some resistance to white noises. The other methods performed slightly worse, which indicates that robustness to adversarial noises comes with a small cost on the accuracy on white-noise corrupted signals.

Under the white-noise attack to the CNN on the CPSC2018 dataset (Fig. 7 (e)–(f)), our method (i.e., “1.0NSR”) performed the best, and the model “CE” performed much worse. The model “24.0Jacob” performed closely to the model “1.0NSR”. A rather surprising result is that the accuracy of the “adv  $\epsilon$ ” models dropped significantly as the white noise level increased, and the performance of the “adv  $\epsilon$ ” models was even not as good as those in the 100-PGD evaluation. The reason could be that an adversarially-trained model is only good at resisting the adversarial noises generated from the same type of adversarial attack, and the regularization-based methods are not tied to a specific type of attack.

## 4. Discussion

We experimentally evaluated the proposed method along with two other methods by using the 100-PGD adversarial attack that is widely used for adversarial robustness research [9,15,24,33], and using the 100-SAP attack that was designed specifically to generate smoothed adversarial ECG samples. Compared to other white-box adversarial attacks, such as DeepFool [34] and C&W [35] attack, the noise level can be controlled in the PGD and SAP algorithms so that the robustness of a model on different noise levels can be investigated.

The adversarial training method used the adversarial samples generated by the PGD attack during the training stage. Our NSR method and the Jacobian method used the PGD attack for parameter tuning. During the testing stage, the three methods were evaluated against not only the PGD attack but also the SAP attack. The results show that the three methods can defend against the SAP attack that is unseen to the methods during training, and our method is the best. PGD is widely used for method evaluation (see Refs. [9,15,24,33]). A recent study [36] compared adversarial attacks and the results show that PGD is the strongest attack. Thus, if a method can defend against the PGD attack, then it is highly likely that it can defend against other unknown adversarial attacks.

After the best parameters are found through the training-validation trials, the performance of every trained model was evaluated on the test set, which ensures the fairness of the comparison. Every defense method has parameters that need to be tuned for a specific dataset, and the tuning process is explained in Section 3.2. The parameter tuning process is indeed time-consuming and currently cannot be avoided, which is a limitation of the current defense methods. Future work in this field needs to focus on developing methods that do not need parameter tuning.

In general, our method performed the best on the two datasets under the 100-PGD attack and the 100-SAP attack. Under the white-noise attack within the noise level of 0.1, the models trained with standard cross-entropy performed the best on the MIT-BIH dataset and much worse on the CPSC2018 dataset, and the models trained by our method performed slightly worse on MIT-BIH dataset and the best on the CPSC2018 dataset. Thus, the results demonstrate that our method can significantly enhance DNN robustness for the application of ECG signal classification, much better than the other two methods that are originally designed for image classification applications. To our best knowledge, our work is the first to improve adversarial robustness of DNNs for ECG signal classification, and neither adversarial training nor Jacobian Regularization has been applied for ECG signal classification.

By definition [25], adversarial noise is small in magnitude but leads to a large change in the model output. Thus, for method evaluation, we only need to focus on a limited range of noise levels. On the MIT-BIH dataset, when the noise level of the PGD-based adversarial attack is higher than 0.1, the adversarial samples/signals are hardly recognizable by the human eye (see Fig. 4). On the CPSC2018 dataset, when the noise level is higher than 0.01, the noises in the adversarial samples/signals become noticeable by the human eye (see Fig. 5), and the performance of the methods dropped sharply after this noise level. In other words, it is much harder to train a robust model for the CPSC2018 dataset. The difficulty of improving model robustness on the CPSC2018 dataset is caused by data annotation/labeling and the sample size. The MIT-BIH dataset has been labeled beat-by-beat, and therefore, we could do classification on the beat level with plenty of training samples (87554). The CPSC2018 dataset only has class labels on the recording level, and therefore there is a limited number of training samples (5905). In general, a DNN model trained with a larger number of samples will have a higher accuracy. Our recent work shows that training sample size may affect adversarial robustness [37]: a larger training set may lead to a higher robustness. Thus, robustness could be further improved on the CPSC2018 dataset if the ECG recordings could be annotated beat-by-beat by human-expert cardiologists.

## 5. Conclusion

In this paper, we proposed a novel regularization method to improve the adversarial robustness of DNNs for ECG signal classification. Our method aims to reduce noise-to-signal ratio (NSR) i.e., reducing the effect of noise on DNN output in order to improve the robustness against adversarial attacks. We evaluated our method on two public datasets, MIT-BIH and CPSC2018, and compared our method with two popular defense methods (Jacobian regularization and PGD-based adversarial

training) that are originally developed for image classification applications. The experimental results have demonstrated that our method outperforms the other two methods under the PGD and SAP adversarial attacks for ECG signal classification. We hope that our approach may facilitate the development of robust applications for automated ECG diagnosis.

## Data availability

The code of this study is publicly available at  
[https://github.com/SarielMa/Robust\\_DNN\\_for\\_ECG](https://github.com/SarielMa/Robust_DNN_for_ECG).

## Appendix A. Tables

**Table 1 A**

Accuracy of MLP “ $\beta$  NSR” on MIT-BIT validation set

	0	0.01	0.03	0.05	0.1	0.2	0.3	ACC <sub>robust</sub>
0.1NSR	89.59%	84.31%	73.74%	63.28%	42.07%	18.10%	11.26%	76.04%
0.2NSR	90.47%	86.16%	82.39%	77.91%	67.42%	45.39%	25.61%	84.03%
0.3NSR	90.36%	84.63%	76.08%	64.99%	48.02%	30.69%	19.75%	77.91%
0.4NSR	90.18%	86.06%	83.72%	81.26%	73.30%	55.80%	40.36%	85.43%
0.5NSR	90.55%	85.41%	77.36%	71.82%	59.32%	36.31%	25.01%	81.18%
0.6NSR	91.00%	85.74%	77.85%	66.74%	50.23%	29.96%	16.74%	79.18%
0.7NSR	91.32%	83.73%	71.18%	59.85%	39.89%	17.25%	7.33%	75.42%
0.8NSR	90.63%	84.35%	79.59%	74.47%	59.16%	32.20%	20.36%	81.87%
0.9NSR	90.44%	82.79%	65.26%	55.00%	48.75%	38.08%	29.10%	74.54%

**Table 1 B**

Accuracy of CNN “ $\beta$  NSR” on MIT-BIT validation set

	0	0.01	0.03	0.05	0.1	0.2	0.3	ACC <sub>robust</sub>
0.1NSR	94.10%	91.17%	88.96%	85.09%	68.10%	32.80%	20.45%	88.36%
0.2NSR	93.67%	88.58%	82.58%	73.90%	58.37%	30.74%	15.14%	83.79%
0.3NSR	93.79%	91.62%	89.53%	87.08%	73.65%	39.44%	22.03%	89.40%
0.4NSR	94.87%	91.47%	86.08%	77.30%	53.03%	32.78%	19.52%	84.91%
0.5NSR	93.62%	89.87%	86.27%	80.92%	60.20%	27.96%	17.73%	85.88%
0.6NSR	93.95%	91.72%	88.69%	84.87%	69.24%	40.61%	25.07%	88.41%
0.7NSR	93.87%	90.72%	89.29%	86.91%	71.77%	41.24%	23.56%	89.07%
0.8NSR	92.95%	88.10%	82.48%	73.56%	57.07%	28.18%	17.13%	83.14%
0.9NSR	92.53%	89.00%	85.99%	82.94%	68.56%	39.39%	23.63%	86.76%

**Table 1 C**

Accuracy of CNN “ $\beta$  NSR” on CPSC2018 validation set

	0	0.001	0.003	0.005	0.007	0.01	0.03	0.05	0.1	ACC <sub>robust</sub>
0.4NSR	73.33%	73.33%	73.33%	71.11%	66.67%	55.56%	11.11%	6.67%	2.22%	70.90%
0.6NSR	77.78%	77.78%	77.78%	75.56%	73.33%	62.22%	24.44%	11.11%	0.00%	75.81%
0.8NSR	77.78%	77.78%	77.78%	77.78%	73.33%	64.44%	31.11%	15.56%	6.67%	76.21%
0.9NSR	73.33%	73.33%	73.33%	68.89%	62.22%	53.33%	26.67%	8.89%	0.00%	69.92%
1.0NSR	93.33%	88.89%	86.67%	86.67%	84.44%	73.33%	26.67%	6.67%	0.00%	88.95%
1.1NSR	66.67%	66.67%	64.44%	62.22%	62.22%	53.33%	22.22%	15.56%	2.22%	64.41%
1.2NSR	37.78%	37.78%	37.78%	37.78%	37.78%	37.78%	35.56%	35.56%	17.78%	37.78%

**Table 2 A**

Accuracy of MLP “ $\lambda$  Jacob” on MIT-BIT validation set

	0	0.01	0.03	0.05	0.1	0.2	0.3	ACC <sub>robust</sub>
0.5Jacob	90.09%	87.44%	78.26%	68.63%	26.88%	1.68%	0.02%	75.94%
0.6Jacob	89.78%	87.47%	79.69%	70.62%	30.61%	2.28%	0.02%	76.93%
0.7Jacob	89.11%	86.35%	79.40%	70.40%	32.38%	3.46%	0.03%	76.70%
0.8Jacob	88.60%	86.45%	78.67%	70.64%	31.50%	3.33%	0.07%	76.31%
0.9Jacob	88.27%	85.63%	79.35%	71.23%	36.62%	3.58%	0.05%	77.03%
1.0Jacob	87.09%	84.91%	78.99%	71.15%	38.91%	6.10%	0.39%	76.68%

(continued on next page)

**Table 2 A (continued)**

	0	0.01	0.03	0.05	0.1	0.2	0.3	ACC <sub>robust</sub>
1.1Jacob	86.30%	84.51%	78.77%	71.72%	43.09%	4.40%	0.13%	76.95%
1.2Jacob	85.66%	83.55%	78.07%	71.71%	43.61%	7.18%	0.50%	76.56%
1.3Jacob	85.54%	83.48%	78.10%	72.02%	44.26%	7.56%	0.55%	76.66%
1.4Jacob	85.15%	82.68%	77.14%	71.56%	44.59%	6.32%	0.28%	76.25%
1.5Jacob	84.94%	82.96%	77.24%	71.92%	46.70%	7.96%	0.78%	76.55%

**Table 2 B**

Accuracy of CNN “λ Jacob” on MIT-BIT validation set

	0	0.01	0.03	0.05	0.1	0.2	0.3	ACC <sub>robust</sub>
0.5Jacob	89.99%	87.99%	82.44%	74.53%	41.60%	1.41%	0.01%	79.75%
0.6Jacob	89.41%	87.64%	81.86%	74.08%	45.07%	1.41%	0.01%	79.78%
0.7Jacob	89.08%	86.96%	81.85%	74.37%	51.79%	2.05%	0.01%	80.56%
0.8Jacob	88.99%	86.55%	81.87%	74.91%	51.39%	3.91%	0.18%	80.53%
0.9Jacob	87.72%	86.14%	81.50%	75.22%	52.21%	5.93%	0.02%	80.02%
1.0Jacob	87.81%	86.12%	81.58%	75.07%	53.00%	4.74%	0.06%	80.14%
1.1Jacob	87.97%	85.74%	81.01%	75.07%	50.33%	4.52%	0.06%	79.76%
1.2Jacob	86.85%	84.84%	80.46%	75.40%	50.23%	4.04%	0.06%	79.14%
1.3Jacob	86.23%	84.78%	80.49%	75.85%	56.51%	6.68%	0.37%	79.77%
1.4Jacob	86.45%	85.06%	80.93%	75.93%	57.40%	6.94%	0.25%	80.09%
1.5Jacob	86.07%	84.56%	80.77%	75.93%	54.79%	6.16%	0.04%	79.49%

**Table 2 C**

Accuracy of CNN “λ Jacob” on CPSC2018 validation set

	0	0.001	0.003	0.005	0.007	0.01	0.03	0.05	0.1	ACC <sub>robust</sub>
4.0Jacob	86.67%	82.22%	77.78%	73.33%	62.22%	53.33%	11.11%	2.22%	0.00%	78.14%
14.0Jacob	86.67%	82.22%	82.22%	75.56%	68.89%	62.22%	24.44%	20.00%	0.00%	80.50%
24.0Jacob	86.67%	86.67%	80.00%	80.00%	80.00%	75.56%	31.11%	17.78%	2.22%	83.61%
34.0Jacob	84.44%	82.22%	80.00%	80.00%	75.56%	71.11%	35.56%	20.00%	0.00%	81.22%
44.0Jacob	86.67%	84.44%	80.00%	77.78%	71.11%	68.89%	44.44%	28.89%	2.22%	81.51%
54.0Jacob	82.22%	80.00%	80.00%	77.78%	75.56%	75.56%	44.44%	24.44%	0.00%	80.03%
64.0Jacob	82.22%	82.22%	82.22%	77.78%	71.11%	68.89%	40.00%	26.67%	4.44%	79.34%
74.0Jacob	80.00%	80.00%	77.78%	75.56%	73.33%	71.11%	46.67%	28.89%	4.44%	77.80%
84.0Jacob	73.33%	73.33%	73.33%	71.11%	68.89%	66.67%	35.56%	31.11%	2.22%	72.04%

**Table 3 A**

Accuracy of MLP “adv ε” on MIT-BIT validation set

	0	0.01	0.03	0.05	0.1	0.2	0.3	ACC <sub>robust</sub>
adv0.05	92.60%	90.73%	85.09%	75.22%	23.47%	0.05%	0.00%	79.03%
adv0.15	90.04%	71.24%	65.75%	64.77%	59.14%	3.94%	0.07%	76.97%
adv0.1	91.82%	80.13%	71.85%	69.57%	57.18%	1.62%	0.03%	79.95%
adv0.25	89.37%	60.07%	44.60%	45.63%	43.65%	9.76%	1.00%	66.36%
adv0.2	89.75%	62.46%	48.41%	47.95%	47.70%	8.32%	0.73%	68.47%
adv0.3	90.50%	58.36%	41.74%	40.07%	38.78%	15.76%	1.60%	64.06%

**Table 3 B**

Accuracy of CNN “adv ε” on MIT-BIT validation set

	0	0.01	0.03	0.05	0.1	0.2	0.3	ACC <sub>robust</sub>
adv0.05	93.36%	91.88%	87.95%	82.31%	30.19%	0.07%	0.00%	82.21%
adv0.15	93.41%	81.89%	79.00%	75.19%	62.34%	3.21%	0.20%	83.51%
adv0.1	91.80%	90.50%	87.44%	83.28%	64.93%	1.05%	0.11%	86.25%
adv0.25	94.85%	80.71%	35.16%	18.10%	6.65%	4.12%	0.98%	54.99%
adv0.2	93.68%	83.91%	63.99%	57.47%	40.75%	7.41%	0.30%	75.20%
adv0.3	94.22%	77.79%	25.90%	7.15%	6.92%	1.07%	0.49%	49.29%

**Table 3 C**

Accuracy of CNN "adv e" on CPSC2018 validation set

	0	0.001	0.003	0.005	0.007	0.01	0.03	0.05	0.1	$ACC_{robust}$
adv0.005	82.22%	80.00%	75.56%	68.89%	62.22%	48.89%	8.89%	0.00%	0.00%	74.71%
adv0.01	84.44%	84.44%	80.00%	73.33%	71.11%	64.44%	13.33%	2.22%	0.00%	<b>79.58%</b>
adv0.02	84.44%	80.00%	75.56%	73.33%	66.67%	62.22%	31.11%	6.67%	0.00%	77.97%
adv0.03	75.56%	75.56%	73.33%	68.89%	68.89%	68.89%	42.22%	17.78%	2.22%	73.30%
adv0.04	68.89%	64.44%	62.22%	55.56%	57.78%	55.56%	42.22%	31.11%	4.44%	63.99%
adv0.05	62.22%	60.00%	55.56%	53.33%	57.78%	53.33%	40.00%	28.89%	13.33%	59.20%
adv0.06	68.89%	62.22%	62.22%	53.33%	55.56%	51.11%	42.22%	35.56%	17.78%	62.91%
adv0.07	57.78%	53.33%	48.89%	44.44%	44.44%	44.44%	37.78%	28.89%	17.78%	52.30%
adv0.08	60.00%	60.00%	51.11%	51.11%	46.67%	48.89%	37.78%	35.56%	24.44%	55.56%
adv0.09	62.22%	55.56%	53.33%	46.67%	42.22%	48.89%	37.78%	35.56%	24.44%	55.40%
adv0.1	42.22%	42.22%	37.78%	35.56%	35.56%	33.33%	26.67%	26.67%	20.00%	39.52%

**Table 4 A**

Accuracy of MLP models on MIT-BIT test set

	0	0.01	0.03	0.05	0.1	0.2	0.3	$ACC_{robust}$
adv0.1	90.87%	81.04%	75.43%	73.40%	57.07%	1.41%	0.01%	80.74%
adv0.2	89.42%	68.73%	60.79%	58.55%	50.95%	9.39%	0.87%	73.35%
adv0.3	89.91%	67.21%	44.89%	39.56%	32.82%	12.29%	0.84%	64.03%
0.9Jacob	87.20%	84.60%	78.50%	70.94%	38.48%	3.69%	0.07%	76.55%
CE	92.16%	69.74%	18.65%	1.86%	0.00%	0.00%	0.00%	42.34%
0.4NSR	89.99%	86.86%	84.35%	81.92%	73.43%	55.27%	40.14%	<b>85.60%</b>

Note: under 100-PGD attack.

**Table 4 B**

F1 of MLP models on MIT-BIT test set

	0	0.01	0.03	0.05	0.1	0.2	0.3	$F1_{robust}$
adv0.1	90.93%	81.28%	75.77%	73.76%	57.67%	1.42%	0.01%	80.98%
adv0.2	89.55%	68.46%	61.32%	59.34%	52.21%	9.94%	0.80%	73.81%
adv0.3	90.04%	67.95%	44.93%	40.25%	34.12%	13.69%	0.92%	64.57%
0.9Jacob	87.29%	84.72%	78.66%	71.15%	39.34%	4.10%	0.06%	76.79%
CE	92.19%	70.14%	19.58%	2.63%	0.01%	0.00%	0.00%	42.91%
0.4NSR	90.16%	87.21%	84.75%	82.38%	74.11%	55.88%	40.23%	<b>85.93%</b>

Note: under 100-PGD attack.

**Table 4 C**

Accuracy of CNN models on MIT-BIT test set

	0	0.01	0.03	0.05	0.1	0.2	0.3	$ACC_{robust}$
adv0.1	91.17%	89.96%	86.47%	82.69%	64.74%	0.65%	0.06%	85.66%
adv0.2	91.91%	74.36%	65.09%	58.69%	45.75%	6.03%	0.40%	74.72%
adv0.3	93.23%	82.22%	33.03%	14.49%	13.48%	2.58%	0.40%	54.66%
0.7Jacob	88.53%	86.17%	81.15%	74.52%	50.11%	2.20%	0.00%	79.94%
CE	93.83%	76.34%	17.71%	1.56%	0.00%	0.00%	0.00%	43.57%
0.3NSR	93.33%	90.58%	88.75%	86.00%	72.36%	38.99%	22.02%	<b>88.64%</b>

Note: under 100-PGD attack.

**Table 4 D**

F1 of CNN models on MIT-BIT test set

	0	0.01	0.03	0.05	0.1	0.2	0.3	$F1_{robust}$
adv0.1	91.21%	90.02%	86.59%	82.85%	65.13%	0.65%	0.05%	85.77%
adv0.2	91.93%	74.52%	64.83%	58.48%	45.73%	6.11%	0.37%	74.67%
adv0.3	93.24%	82.34%	31.83%	14.73%	14.37%	2.73%	0.34%	54.73%
0.7Jacob	88.55%	86.20%	81.13%	74.38%	49.81%	2.52%	0.00%	79.88%
CE	93.83%	76.54%	19.19%	2.08%	0.00%	0.00%	0.00%	44.11%
0.3NSR	93.36%	90.61%	88.77%	86.03%	72.07%	35.05%	14.20%	<b>88.63%</b>

Note: under 100-PGD attack.

**Table 4 E**

Accuracy of CNN models on CPSC2018 test set

	0	0.001	0.003	0.005	0.007	0.01	0.03	0.05	0.1	$ACC_{robust}$
adv0.005	83.78%	82.44%	77.11%	71.56%	65.33%	50.22%	7.78%	1.33%	0.00%	76.66%
adv0.01	82.67%	82.00%	79.33%	75.56%	72.22%	63.56%	22.44%	6.89%	0.89%	78.74%
adv0.05	73.11%	69.78%	65.33%	61.78%	60.22%	57.33%	47.33%	39.56%	19.33%	67.98%
adv0.1	62.89%	59.33%	57.56%	52.89%	52.44%	50.67%	44.00%	42.89%	32.00%	58.73%
CE	79.56%	63.33%	27.33%	8.89%	2.89%	0.44%	0.00%	0.00%	0.00%	41.37%
1.0NSR	83.33%	82.00%	79.56%	77.33%	72.89%	67.33%	30.22%	14.89%	3.56%	<b>79.67%</b>
24.0Jacob	82.22%	80.44%	77.56%	75.78%	72.44%	67.33%	37.56%	19.56%	2.00%	78.56%

Note: under 100-PGD attack.

**Table 4 F**

F1 of CNN models on CPSC2018 test set

	0	0.001	0.003	0.005	0.007	0.01	0.03	0.05	0.1	$F1_{robust}$
adv0.005	83.33%	82.05%	76.49%	70.58%	64.08%	48.93%	6.76%	1.00%	0.00%	75.96%
adv0.01	82.10%	81.38%	78.70%	74.58%	71.20%	62.36%	22.61%	7.42%	0.92%	78.01%
adv0.05	71.58%	68.45%	63.92%	60.54%	59.37%	56.75%	47.86%	40.78%	20.86%	66.67%
adv0.1	61.97%	58.79%	57.15%	53.11%	52.70%	51.16%	44.93%	44.08%	33.31%	58.29%
CE	78.99%	62.40%	27.23%	9.74%	3.12%	0.60%	0.00%	0.00%	0.00%	41.28%
1.0NSR	83.04%	81.78%	79.27%	76.83%	72.23%	66.32%	29.15%	14.80%	4.12%	<b>79.26%</b>
24.0Jacob	81.85%	79.96%	76.81%	75.11%	71.72%	66.87%	37.90%	20.95%	2.02%	78.05%

Note: under 100-PGD attack.

**Table 5 A**

Accuracy of MLP models on MIT-BIT test set

	0	0.01	0.03	0.05	0.1	0.2	0.3	$ACC_{robust}$
adv0.1	90.87%	75.88%	61.39%	49.30%	24.47%	0.88%	0.07%	68.46%
adv0.2	89.42%	42.00%	31.88%	23.25%	11.65%	1.51%	0.78%	50.21%
adv0.3	89.91%	48.08%	22.35%	14.75%	5.04%	0.67%	0.10%	45.08%
0.9Jacob	87.20%	85.10%	80.55%	74.69%	50.25%	7.26%	0.95%	79.20%
CE	92.16%	82.56%	41.13%	20.37%	1.62%	0.00%	0.00%	54.94%
0.4NSR	89.99%	87.23%	85.57%	84.26%	81.15%	74.60%	64.01%	<b>87.19%</b>

Note: under 100-SAP attack.

**Table 5 B**

F1 of MLP models on MIT-BIT test set

	0	0.01	0.03	0.05	0.1	0.2	0.3	$F1_{robust}$
adv0.1	90.93%	76.03%	62.36%	51.34%	26.35%	1.00%	0.07%	69.41%
adv0.2	89.55%	40.05%	30.48%	23.32%	12.75%	1.40%	0.44%	50.01%
adv0.3	90.04%	47.57%	21.72%	15.01%	5.84%	0.84%	0.07%	45.21%
0.9Jacob	87.29%	85.21%	80.71%	74.89%	50.90%	7.78%	1.14%	79.40%
CE	92.19%	82.70%	41.03%	21.42%	2.50%	0.00%	0.00%	55.44%
0.4NSR	90.16%	87.55%	85.95%	84.69%	81.57%	75.35%	64.28%	<b>87.47%</b>

Note: under 100-SAP attack.

**Table 5 C**

Accuracy of CNN models on MIT-BIT test set

	0	0.01	0.03	0.05	0.1	0.2	0.3	$ACC_{robust}$
adv0.1	91.34%	90.11%	87.83%	85.04%	73.80%	16.43%	1.56%	87.52%
adv0.2	92.56%	87.27%	67.05%	52.79%	31.90%	4.83%	0.12%	73.01%
adv0.3	93.08%	87.19%	62.59%	31.21%	2.20%	0.01%	0.00%	62.32%
0.7Jacob	88.53%	86.83%	83.27%	78.99%	63.77%	14.92%	0.68%	82.93%
CE	93.38%	84.88%	47.99%	18.00%	2.25%	0.00%	0.00%	56.23%
0.3NSR	93.33%	91.68%	89.84%	88.78%	85.39%	80.48%	77.71%	<b>91.04%</b>

Note: under 100-SAP attack.

**Table 5 D**

F1 of CNN models on MIT-BIT test set

	0	0.01	0.03	0.05	0.1	0.2	0.3	$F1_{robust}$
adv0.1	91.36%	90.14%	87.90%	85.14%	73.91%	18.16%	1.47%	87.57%
adv0.2	92.60%	87.42%	66.96%	51.92%	30.45%	5.78%	0.13%	72.60%
adv0.3	93.09%	87.22%	63.02%	32.11%	1.87%	0.01%	0.00%	62.57%
0.7Jacob	88.55%	86.86%	83.28%	78.98%	63.64%	15.79%	0.74%	82.93%
CE	93.38%	84.91%	48.22%	19.66%	3.26%	0.00%	0.00%	56.96%
0.3NSR	93.36%	91.73%	89.86%	88.83%	85.45%	80.50%	77.68%	<b>91.08%</b>

Note: under 100-SAP attack.

**Table 5 E**

Accuracy of CNN models on CPSC2018 test set

	0	0.001	0.003	0.005	0.007	0.01	0.03	0.05	0.1	$ACC_{robust}$
adv0.01	82.67%	80.44%	78.22%	76.44%	73.78%	70.22%	56.00%	46.44%	31.56%	79.32%
adv0.05	73.11%	57.78%	47.56%	42.89%	39.33%	34.22%	23.33%	19.56%	13.33%	57.60%
adv0.1	62.89%	51.11%	44.44%	39.78%	36.89%	32.89%	21.56%	16.22%	10.89%	51.28%
CE	79.56%	77.56%	71.33%	67.78%	60.67%	55.33%	21.11%	8.00%	1.56%	72.95%
1.0NSR	83.33%	83.33%	83.33%	83.33%	83.11%	82.22%	81.56%	80.00%	73.56%	<b>83.22%</b>
24.0Jacob	82.22%	82.00%	82.00%	81.78%	81.56%	81.33%	80.00%	78.67%	76.67%	81.99%

Note: under 100-SAP attack.

**Table 5 F**

F1 of CNN models on CPSC2018 test set

	0	0.001	0.003	0.005	0.007	0.01	0.03	0.05	0.1	$F1_{robust}$
adv0.01	82.10%	79.88%	77.63%	75.87%	73.11%	69.55%	55.15%	45.82%	31.96%	78.73%
adv0.05	71.58%	56.76%	48.02%	43.87%	40.70%	36.12%	25.49%	21.78%	15.34%	57.42%
adv0.1	61.97%	51.34%	45.42%	40.95%	38.43%	35.08%	24.35%	18.72%	13.00%	51.59%
CE	78.99%	76.87%	70.53%	66.96%	59.97%	54.75%	21.26%	7.63%	1.68%	72.30%
1.0NSR	83.04%	83.04%	83.04%	83.04%	82.82%	81.98%	81.31%	79.71%	73.31%	<b>82.93%</b>
24.0Jacob	81.85%	81.56%	81.56%	81.34%	81.09%	80.85%	79.51%	78.05%	75.95%	81.58%

Note: under 100-SAP attack.

**Table 6 A**

Accuracy of MLP models on MIT-BIT test set

	0	0.01	0.03	0.05	0.1	0.2	0.3	$ACC_{robust}$
adv0.1	90.87%	90.87%	90.54%	89.04%	87.62%	86.79%	86.38%	90.11%
adv0.2	89.42%	89.42%	88.99%	84.26%	83.00%	82.14%	81.78%	87.65%
adv0.3	89.91%	89.91%	89.34%	83.18%	81.49%	80.15%	79.83%	87.59%
0.9Jacob	87.20%	87.20%	87.06%	86.73%	86.25%	84.92%	83.09%	86.99%
CE	92.16%	92.16%	92.34%	91.52%	89.67%	80.73%	69.36%	<b>91.75%</b>
0.4NSR	89.99%	89.99%	89.84%	89.49%	88.77%	85.27%	79.62%	89.74%

Note: under White-noise attack.

**Table 6 B**

F1 of MLP models on MIT-BIT test set

	0	0.01	0.03	0.05	0.1	0.2	0.3	$F1_{robust}$
adv0.1	90.93%	90.93%	90.56%	89.07%	87.73%	86.95%	86.54%	90.16%
adv0.2	89.55%	89.55%	89.00%	84.50%	83.36%	82.50%	82.14%	87.82%
adv0.3	90.04%	90.04%	89.41%	83.31%	81.69%	80.24%	79.85%	87.73%
0.9Jacob	87.29%	87.29%	87.15%	86.82%	86.36%	85.05%	83.26%	87.08%
CE	92.19%	92.19%	92.38%	91.58%	89.78%	80.88%	69.07%	<b>91.80%</b>
0.4NSR	90.16%	90.16%	90.02%	89.68%	89.00%	85.63%	79.93%	89.92%

Note: under White-noise attack.

**Table 6 C**

Accuracy of CNN models on MIT-BIT test set

	0	0.01	0.03	0.05	0.1	0.2	0.3	$ACC_{robust}$
adv0.1	91.17%	91.17%	91.21%	91.10%	91.10%	90.74%	89.17%	91.16%
adv0.2	91.91%	91.91%	92.23%	86.30%	85.69%	85.37%	85.11%	90.17%
adv0.3	93.23%	93.23%	93.12%	92.40%	89.83%	82.12%	81.47%	92.65%
0.7Jacob	88.53%	88.53%	88.39%	88.12%	87.79%	86.81%	85.68%	88.35%

(continued on next page)

**Table 6 C (continued)**

	0	0.01	0.03	0.05	0.1	0.2	0.3	$ACC_{robust}$
CE	93.83%	93.83%	93.79%	93.18%	91.96%	85.94%	74.31%	<b>93.47%</b>
0.3NSR	93.33%	93.33%	93.14%	92.47%	91.08%	84.64%	72.47%	92.88%

Note: under White-noise attack.

**Table 6 D**

F1 of CNN models on MIT-BIT test set

	0	0.01	0.03	0.05	0.1	0.2	0.3	$F1_{robust}$
adv0.1	91.21%	91.21%	91.24%	91.13%	91.13%	90.78%	89.24%	91.19%
adv0.2	91.93%	91.93%	92.27%	86.45%	85.86%	85.54%	85.29%	90.23%
adv0.3	93.24%	93.24%	93.13%	92.43%	90.00%	82.43%	81.74%	92.68%
0.7Jacob	88.55%	88.55%	88.41%	88.15%	87.81%	86.83%	85.71%	88.37%
CE	93.83%	93.83%	93.79%	93.18%	91.99%	86.13%	74.35%	<b>93.48%</b>
0.3NSR	93.36%	93.36%	93.17%	92.51%	91.12%	84.79%	72.46%	92.91%

Note: under White-noise attack.

**Table 6 E**

Accuracy of CNN models on CPSC2018 test set

	0	0.05	0.1	0.2	0.3	$ACC_{robust}$
adv0.01	82.67%	80.22%	77.33%	74.44%	70.00%	75.40%
adv0.05	73.11%	58.67%	56.67%	55.78%	55.56%	63.60%
adv0.1	62.89%	48.89%	46.89%	42.44%	42.67%	51.95%
CE	79.56%	75.11%	69.33%	63.33%	56.67%	67.95%
1.0NSR	83.33%	83.33%	82.44%	80.89%	78.22%	<b>79.92%</b>
24.0Jacob	82.22%	80.93%	80.45%	78.34%	76.68%	79.48%

Note: under White-noise attack.

**Table 6 F**

F1 of CNN models on CPSC2018 test set

	0	0.05	0.1	0.2	0.3	$F1_{robust}$
adv0.01	82.10%	79.78%	77.06%	74.49%	70.17%	75.20%
adv0.05	71.58%	58.28%	56.58%	55.64%	55.63%	62.91%
adv0.1	61.97%	49.32%	47.49%	42.97%	43.31%	51.75%
CE	79.56%	75.11%	69.33%	63.33%	56.67%	67.95%
1.0NSR	83.04%	83.04%	82.19%	80.61%	77.91%	<b>79.50%</b>
24.0Jacob	81.85%	80.93%	80.45%	78.34%	76.68%	79.29%

Note: under White-noise attack.

**Table 7 A**

Accuracy of MLP models on MIT-BIT validation set, with different optimizers and learning rate (using the cross-entropy loss)

Learning Rate	0.1	0.01	0.001	0.0001
Adam	66.29%	92.42%	91.83%	89.31%
Adamax	81.77%	90.09%	<b>92.95%</b>	91.51%
SGD	80.97%	89.36%	89.2%	88.9%

**Table 7 B**

Accuracy of CNN models on MIT-BIT validation set, with different optimizers and learning rate (using the cross-entropy loss)

Learning Rate	0.1	0.01	0.001	0.0001
Adam	20%	90.01%	94.47%	92.88%
Adamax	87.47%	93.73%	<b>95.33%</b>	91.72%
SGD	20%	93.65%	94.58%	93.36%

**Table 7 C**

Accuracy of CNN models on CPSC2018 validation set, with different optimizers and learning rate (using the cross-entropy loss)

Learning Rate	0.1	0.01	0.001	0.0001
Adam	11.11%	80.00%	<b>82.00%</b>	80.67%
Adamax	75.56%	77.78%	77.78%	77.78%
SGD	77.78%	77.78%	77.78%	75.56%

## Appendix B

The  $F1_{robust}$  is defined by:

$$F1_{robust} = \sqrt{F1_{clean} \times AUC_{\|\delta\|_\infty \leq \varepsilon_{max}}}$$

Here,  $F1_{clean}$  is the classification F1 score on clean data (without adversarial noises).  $AUC_{\|\delta\|_\infty \leq \varepsilon_{max}}$  is the normalized area under the curve of F1 score vs. noise level, which is the average classification F1 score computed across a range of noise levels, i.e.,  $\|\delta\|_\infty \leq \varepsilon_{max}$ .

## References

- [1] Y. LeCun, Y. Bengio, G. Hinton, Deep learning, *Nature* 521 (7553) (May 28 2015) 436–444.
- [2] S.H. Jambukia, V.K. Dabhi, H.B. Prajapati, Classification of ECG signals using machine learning techniques: a survey, in: International Conference on Advances in Computer Engineering and Applications, IEEE, 2015, pp. 714–721.
- [3] A. Lyon, A. Mincholé, J.P. Martínez, P. Laguna, B. Rodriguez, Computational techniques for ECG analysis and interpretation in light of their contribution to medical advances, *J. R. Soc. Interface* 15 (138) (2018), 20170821.
- [4] S. Hong, Y. Zhou, J. Shang, C. Xiao, J. Sun, Opportunities and Challenges of Deep Learning Methods for Electrocardiogram Data: A Systematic Review," *Computers in Biology Medicine*, 2020, p. 103801.
- [5] S. Kiranyaz, T. Ince, M. Gabbouj, Real-time patient-specific ECG classification by 1-D convolutional neural networks, *IEEE Trans. Biomed. Eng.* 63 (3) (2015) 664–675.
- [6] P. Rajpurkar, A.Y. Hannun, M. Haghpanahi, C. Bourn, A. Ng, Cardiologist-Level Arrhythmia Detection With Convolutional Neural Networks, 2017 arXiv preprint arXiv:1707.01836.
- [7] N. Akhtar, A. Mian, Threat of adversarial attacks on deep learning in computer vision: a survey, *IEEE Access* 6 (2018) 14410–14430.
- [8] I.J. Goodfellow, J. Shlens, C. Szegedy, Explaining And Harnessing Adversarial Examples, 2014 arXiv preprint arXiv:1412.6572.
- [9] A. Madry, A. Makelov, L. Schmidt, D. Tsipras, A. Vladu, Towards deep learning models resistant to adversarial attacks, in: International Conference on Learning Representations, 2018.
- [10] N. Papernot, P. McDaniel, I. Goodfellow, S. Jha, Z.B. Celik, A. Swami, Practical black-box attacks against machine learning, in: Proceedings of the 2017 ACM on Asia Conference on Computer and Communications Security, 2017, pp. 506–519.
- [11] J. Uesato, B. O’donoghue, P. Kohli, A. Oord, Adversarial risk and the dangers of evaluating against weak attacks, in: International Conference on Machine Learning, PMLR, 2018, pp. 5025–5034.
- [12] X. Han, Y. Hu, L. Foschini, L. Chinitz, L. Jankelson, R. Ranganath, Deep learning models for electrocardiograms are susceptible to adversarial attack, *Nat. Med.* 26 (3) (2020) 360–363.
- [13] S. Benjamins, P. Dhunnoo, B. Meskó, The state of artificial intelligence-based FDA-approved medical devices and algorithms: an online database, *NPJ Digit. Med.* 3 (2020).
- [14] A. Kurakin, et al., Adversarial Attacks and Defences Competition, Springer International Publishing, Cham, 2018, pp. 195–231.
- [15] F. Tramer, N. Carlini, W. Brendel, A. Madry, On adaptive attacks to adversarial example defenses, in: Conference on Neural Information Processing Systems, 2020.
- [16] H. Zhang, Y. Yu, J. Jiao, E. Xing, L. El Ghaoui, M. Jordan, Theoretically principled trade-off between robustness and accuracy, in: International Conference on Machine Learning, PMLR, 2019, pp. 7472–7482.
- [17] A. Ross, F. Doshi-Velez, Improving the adversarial robustness and interpretability of deep neural networks by regularizing their input gradients, *Assoc. Adv. Artif. Intell.* 32 (2018) 1.
- [18] D. Jakubovitz, R. Giryes, Improving dnn robustness to adversarial attacks using jacobian regularization, in: European Conference on Computer Vision, 2018, pp. 514–529.
- [19] G.B. Moody, R. Mark, B. Magazine, The impact of the MIT-BIH arrhythmia database, *IEEE Engineering in Medicine and Biology Magazine* 20 (3) (2001) 45–50.
- [20] The China Physiological Signal Challenge 2018, in: The 7th International Conference on Biomedical Engineering and Biotechnology, 2018. Available: <http://2018.icbeb.org/Challenge.html>.
- [21] F. Liu, et al., An open access database for evaluating the algorithms of electrocardiogram rhythm and morphology abnormality detection, *J. Med. Imaging Health Inf.* 8 (7) (2018) 1368–1373.
- [22] L. Ma, L. Liang, Enhance CNN Robustness against Noises for Classification of 12-Lead ECG with Variable Length, in: The 19th IEEE International Conference on Machine Learning and Applications, IEEE, 2020, pp. 839–846.
- [23] L. Ma, L. Liang, Improve robustness of DNN for ECG signal classification: a noise-to-signal ratio perspective, in: International Conference on Learning Representations Workshop AI for Affordable Health, 2020.
- [24] G.W. Ding, Y. Sharma, K.Y.C. Lui, R. Huang, Mma training: direct input space margin maximization through adversarial training, in: International Conference on Learning Representations, 2020.
- [25] I. Goodfellow, P. McDaniel, N. Papernot, Making machine learning robust against adversarial inputs, *Commun. ACM* 61 (7) (2018) 56–66.
- [26] M. Kachuee, S. Fazeli, M. Sarrafzadeh, Ecg heartbeat classification: a deep transferable representation, in: 2018 IEEE International Conference on Healthcare Informatics (ICHI), IEEE, 2018, pp. 443–444.
- [27] Y. Wu, K. He, Group normalization, in: Proceedings of the European Conference on Computer Vision, 2018, pp. 3–19.
- [28] ECG Heartbeat Categorization Dataset, Kaggle, 2018. Available: <https://www.kaggle.com/shayanfazeli/heartbeat>.
- [29] Association for the Advancement of Medical Instrumentation, Testing and Reporting Performance Results of Cardiac Rhythm and ST Segment Measurement Algorithms, ANSI/AAMI EC38, 1998.
- [31] 12-Lead ECG monitoring with EASI™ lead system, Available: [https://www.theonlinlearningcenter.com/Assets/PMDCBT/PIIC\\_Fundamentals\\_1.0/shell/viewer/swfs/assets/downloads/easi.pdf](https://www.theonlinlearningcenter.com/Assets/PMDCBT/PIIC_Fundamentals_1.0/shell/viewer/swfs/assets/downloads/easi.pdf).
- [32] F. Pedregosa, et al., Scikit-learn: machine learning in Python, *J. Mach. Learn. Res.* 12 (2011) 2825–2830.
- [33] A. Shafahi, et al., Adversarial training for free, in: Conference on Neural Information Processing Systems, 2019.
- [34] S.-M. Moosavi-Dezfooli, A. Fawzi, P. Frossard, Deepfool: a simple and accurate method to fool deep neural networks, in: Proceedings of the IEEE Conference on Computer Vision and Pattern Recognition, 2016, pp. 2574–2582.
- [35] N. Carlini, D. Wagner, Adversarial examples are not easily detected: Bypassing ten detection methods, in: Proceedings of the 10th ACM Workshop on Artificial Intelligence and Security, 2017, pp. 3–14.
- [36] J. Wu, M. Zhou, C. Zhu, Y. Liu, M. Harandi, L.J.a. p. a. Li, Performance Evaluation of Adversarial Attacks: Discrepancies and Solutions, 2021 arXiv:2104.11103.
- [37] J. Chen, L. Qian, T. Urakov, W. Gu, L. Liang, Adversarial robustness study of convolutional neural network for Lumbar Disk shape reconstruction from MR images, in: SPIE Medical Imaging: Image Processing, 2021.
- [38] Xavier Glorot, Boris Antoine, Yoshua Bengio, Deep sparse rectifier neural networks, in: Proceedings of the Fourteenth International Conference on Artificial Intelligence and Statistics, JMLR Workshop and Conference Proceedings, 2011.
- [39] Raman Arora, et al., Understanding Deep Neural Networks with Rectified Linear Units, in: International Conference on Learning Representations, 2018.
- [40] Boris Hanin, David Rolnick, Deep ReLU Networks Have Surprisingly Few Activation Patterns, in: Advances in Neural Information Processing Systems 32 (NeurIPS 2019), 2019.